Receiver Architectures for MIMO Wireless Communication Systems based on VBLAST and Sphere Decoding Algorithms

Foluwaso Tade

A thesis submitted in partial fulfilment of the requirements of the University

of Hertfordshire for the degree of Doctor of Philosophy

School of Engineering and Technology,
University of Hertfordshire,
College Lane Campus, Hatfield, AL10 9AB

June 2011

Abstract

Modern day technology aspires to always progress. This progression leads to a lot of research in any significant area of improvement. There is a growing amount of end-users in the wireless spectrum which has led to a need for improved bandwidth usage and BER values. In other words, new technologies which would increase the capacity of wireless systems are proving to be a crucial point of research in these modern times.

Different combinations of multiuser receivers are evaluated to determine performance under normal working conditions by comparing their BER performance charts. Multiple input, multiple output (MIMO) systems are incorporated into the system to utilise the increased capacity rates achievable using the MIMO configuration. The effect of MIMO on the technologies associated with modern day technological standards such as CDMA and OFDM have been investigated due to the significant capacity potentials these technologies normally exhibit in a single antenna scenario. An in-depth comparison is established before comparison is made with a conventional maximum likelihood (ML) detector.

The complexity of the ML detector makes its realization evaluated in such a manner to achieve the same or near ML solution but with lower computational complexity. This was achieved using a proposed modification of the Schnorr-Euchner Sphere decoding algorithm (SE-SDA). The proposed sphere decoder (P-SD) adopts a modification of the radius utilised in the SE-SDA to obtain a near ML solution at a much lower complexity compared to the conventional ML decoder. The P-SD was configured to work in different MIMO antenna configurations.

The need for the highest possible data rates from the available limited spectrum led to my research into the multi-user detection scenario and MIMO.

University of Hertfordshire, 2011

Acknowledgements

Firstly, I would like to express my deepest thanks to God for his blessings and directions in giving me the knowledge and health to complete this project.

I would like to say a big THANK YOU to my family; especially my parents, for their support and assistance in every manner towards the completion of this project.

I would like to express my utmost gratitude to my supervisor, Prof. Yichuang Sun. His advice, support, encouragement, motivation, guidance and perseverance were at times priceless and immense. I would also like to say a big THANK YOU to him for his belief in this project and in my completion of the task.

Finally, I would like to say one last THANK YOU to my friends and colleagues. Their belief in me made me attain that belief within myself and served as a catalyst towards the completion of this project.

University of Hertfordshire, 2011

List of Abbreviations

BER   Bit Error Rate

BLAST   Bell Labs Layered Space Time

BS   Base station

CAI   Co-Antenna Interference

CDMA   Code Division Multiple Access

IEEE   Institute of Electrical and Electronics Engineers

i.i.d   Identically independent distribution

ITU   International Telecommunications Union

MAI   Multiple Access Interference

MC   Multi Carrier

MIMO   Multiple input, Multiple output

ML   Maximum Likelihood

MMSE   Minimum Mean Squared Error

MUD   Multiuser Detection

NP-Hard   Non-Deterministic Polynomial Time Hard

OFDM   Orthogonal Frequency Division Multiplexing

PIC   Parallel Interference Cancellation

University of Hertfordshire, 2011

PSK   Phase Shift Keying

QAM   Quadrature Amplitude Modulation

QPSK   Quadrature Phase Shift Keying

SD   Sphere Decoder

SDA   Sphere Decoding Algorithm

S-E   Schnorr-Euchner

SIC   Successive Interference Cancellation

SISO   Single-input Single-output

SNR   Signal-to-Noise ratio

STBC   Space Time Block Code

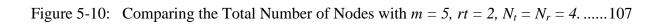WiMaX   Worldwide Interoperability for Microwave Access

WLAN   Wireless Local Area Network

ZF   Zero Forcing

List of Figures

University of Hertfordshire, 2011

University of Hertfordshire, 2011

University of Hertfordshire, 2011

List of Tables

University of Hertfordshire, 2011

Table of Contents

University of Hertfordshire, 2011

University of Hertfordshire, 2011

University of Hertfordshire, 2011

University of Hertfordshire, 2011

1 Introduction

1.1 A General Overview

Wireless communications is an important part of the telecommunications industry. It is easily the fastest growing part of the telecommunications industry. The available resources are limited and therefore maximising how we use it is a very attractive research area. The advent of multiple input, multiple output (MIMO) antennas has had a major influence on how the current capacity limits of single antenna systems could be increased without the need of overwhelming computational complexity. MIMO enhances the capacity of the system and can be used in conjunction with multi-user techniques to improve system throughput. This introductory chapter gives a brief overview of the main elements researched within this project.

1.1.1 Multi-user Detection Techniques

There is a growing amount of end-users in the wireless spectrum which has led to a need for improved bandwidth usage and BER values. In other words, new technologies which would increase the capacity of wireless systems are proving to be a crucial point of research in these modern times. Hence, the focus of the research was to examine, identify and establish a detector capable of delivering rates required by the demand of the end users in modern day telecommunication systems.

Multiuser detection (MUD) is a technique that has been widely accepted in current telecommunications technologies as the demand from the end user increases. It enables the

multiple users to share the same wireless communications channel and therefore increasing overall system capacity. Essentially, MUD can be envisaged as one of the most important breakthroughs achieved in wireless telecommunication technology. The demand caused by the end user led to a lot of users operating within the same frequency allocation as seen in the 3G mobile broadcast cells although they do so at different time intervals. The advent of increased users caused the introduction of multiple access interference (MAI) in mobile wireless systems. MAI is an interference caused by the existence of multiple users allotted to the same frequency range. MAI is witnessed when these users access the allotted frequency band at the same time. In essence, although several users can transmit at the same frequency, MAI would be present provided two or more users are transmitting at the same time. Multiuser detection (MUD) techniques aim to remove the effect of MAI from the wireless system [20].

1.1.2   Multiple Input, Multiple Output (MIMO) Systems

The use of multiple transmit and receive antennas has been proposed for the fourth generation code-division multiple access (CDMA) and orthogonal frequency division multiplex (OFDM) wireless cellular networks in order to meet the increasing demands for higher data rates [7], [8]. MIMO systems are utilised to increase total system data rates, throughput and capacity [9]. MIMO is a simple algorithm which manipulates the *space* dimension of a wireless telecommunication spectrum to achieve increased data rates without the need to add complex software [7], [8], [9]. Prior to MIMO, improved data rates were normally increased by transmitting at higher modulation rates. MIMO system adopts multiple antennas at both the transmitter and the receiver; hence, MIMO simply adds a simple hardware change to the system rather than increased computational complexities as witnessed with using a higher modulation technique [9], [46].

University of Hertfordshire, 2011

1.1.3   The Maximum Likelihood Solution

The function of a receiver can be visualised as a bunch of algorithms working together to correctly predict a received signal that has been corrupted by noise from the wireless channel. The optimal solution of any received signal is generically termed the maximum likelihood (ML) solution for that received signal. This optimal solution raises issues such as the overall exhaustive *runtime* of the system and the burden of iterations required to find the result [20], [46]. These drawbacks make the ML solution termed to be a NP-Hard process [20]. Hence, sub-optimal processes where the performance of the receiver is closest to the performance of ML receiver have been investigated in this research.

Bit error rates (BERs) are a means of analysing and investigating how efficient a receiver performs under certain conditions. BER performance have been computed and analysed for different receiver systems and combinations to establish performance margins in the presence of noise and interference.

1.2   Aims and Objectives

The aims and objectives of this project can be visualised as indicated below.

- To review typical single antenna systems
- To establish the variations of detectors and investigate their BER performance
- To disseminate the MIMO algorithm and investigate the current MIMO detectors
- To identify a suitable MIMO detector and combine it with a multi-user signal to investigate the combination of MUD and MIMO
- To extend the MIMO algorithm to OFDM and CDMA systems to study the effect using the calculated BER performance

- To compare the sphere decoding algorithm (SDA) to the maximum likelihood (ML) detector
- To establish a modification that improves on the utilised SDA

1.3   Thesis Contributions

The novel contributions of this thesis have been highlighted below.

- Devised a clear and precise presentation of the progression from low performance receivers to high performance receivers.
- Implemented a decoding algorithm developed by Foschini [46] using different modulation techniques and antenna configuration.
- Analysed Foschini's decoding algorithm in [46] and the combination with CDMA and OFDM
- Provided a clear and precise description of the sphere decoding algorithm.
- Implemented the receiver algorithm devised by Schnorr and Euchner in [36] and investigated the effect of its combination with MIMO systems using different modulation techniques and antenna configurations.
- Implemented a novel adaptation of a very utilised algorithm for detection in MIMO receivers

University of Hertfordshire, 2011

1.4   Thesis Outline

Chapter 1 is a basic introduction to the work done within the project and gives a brief summary of the main objectives.

Chapter 2 provides an overview of single input, single output (SISO) multiuser systems and identifies the sub-par performance noticed.

Chapter 3 introduces the reader to MIMO with a complete dissemination of the technology by investigating the key components and attributes with regards to single user communications. The BER performance of different MIMO receivers is investigated.

Chapter 4 introduces the concept of MIMO in combination with higher order modulation technologies such as multi-user CDMA and OFDM. Modern telecommunication networks normally adopt these standards so in effect; the combination of MIMO with these technologies was also investigated.

Chapter 5 analyses the ML solution and provides a proper insight into the complexities involved in obtaining this solution. It then proposes a modification to the receiver algorithm developed by Schnorr and Euchner in [36].

Chapter 6 concludes the research project by identifying the benefit of the proposed scheme and highlight significant advantages of adopting the proposed algorithm in modern day wireless systems. It also discusses future work that can be carried out to further the research.

2 Multiuser Detection (MUD) Algorithms

2.1 Introduction

The ultimate aim of the telecommunications industries of today is the transmission and reception of information; voice, data or a combination of both; with high data rates and offering significantly low interference.

Wireless communications is one of the rapidly growing means of communications simply because of the attraction it brings to the end users: **mobility**. Due to technological advancements, the premature use of wireless devices as simply a means of voice communications; as used by mobile phones, needed to be reassessed to accommodate for the growing need for multimedia and text messages. This need created a desire for very high data rates which could not simply be offered due to the limited radio spectrum and signal interference. Although wired devices offer these desired rates, they lack the needed advantages of mobility and instantaneity hence research into achieving these rates for wireless systems became a significant area of research in our modern day world.

The modern day world strives for perfection. This attribute contributes to the need for the maximum data bandwidth, fastest processing speeds and minimum errors. The last attribute is where multiuser detection is involved. It is a combination of techniques employed to minimise the errors in the 'receive' end of a communications system.

MUD is a topic of great interest as the need for higher bandwidths and greater speeds generates a need for receivers that reflect minimum errors. The multi-user detection schemes are simply a combination of algorithms that readily detect the incoming multi-user signals. This property enables different MUD combinations to be serially processed together to

achieve better error rates although the more combinations visualised, the greater the complexity of the system.

This chapter gives a general overview of the most common multi-user detection techniques for use in SISO systems. Different combinations of ZF, MMSE and SIC detectors have been investigated to determine the detector combination most suitable for the final receive detector discussed in Chapter 5.

2.2 Multi-user Detection: A Brief Overview for SISO Systems

Multiuser receivers would never yield a perfect match between the transmitted and received signals [4]. An approximation to a perfect match exists in the Optimal Maximum Likelihood Sequence Estimation Receiver (MLSE). This receiver has its major drawbacks with respect to the computational complexity of the system increasing exponentially with the total number of users [4]. Verdu derived the optimal CDMA receiver in 1986 [4]. This was pre-empted seven years earlier by the introduction of multi-user detection by Schneider in 1979 [4]. The optimal receiver consists of a bank of matched filters which are used to provide first order user amplitude estimates to a Viterbi decision algorithm. Verdu showed mathematically that the optimal receiver gave a very significant performance improvement over the conventional structure, but the expense of its implementation increased significantly with the total number of users in the system. This also raised an issue due to the significant complexity involved in deploying the system. Hence, less expensive and less complex detectors are currently being proposed although the optimal detector is now being used as a benchmark for future systems. To reduce this significant drawback, an estimation of the receiver is considered; this led to the study of 'sub-optimal' receivers. The major formats of multi-user receivers can be envisaged in Figure 2-1.

Multi-user Receiver

Optimal MLSE

Sub-Optimal

Linear

Non-linear

Decorrelator

MMSE

Multi-Stage

Decision Feedback

Successive Interference Cancellation
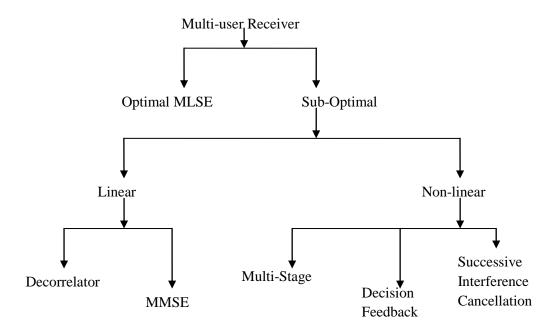
Figure 2-1:   Different MUD Configurations

The different types of receivers possess their corresponding advantages and disadvantages; therefore, an insight into their theoretical behaviour is essential. As shown in Figure 2-1, there are two variations; linear and non-linear receivers. The design tradeoffs which need to be considered when deciding upon any receiver detection algorithms are:

- Near Far Resistance
- Asynchronous versus Synchronous
- Linear versus Non-Linear
- Performance versus Complexity
- Limitations under Practical Operating Conditions

University of Hertfordshire, 2011

2.2.1 Near-Far Resistance

This corresponds to the fact that the receiver picks up the incoming detected signals at different receive powers.

- Signals reach the receiver at different powers; caused by fading, distance from the receiver and different transmit powers of the user (i.e. as seen in the cellular industry).
- Linear receivers are not affected by this phenomenon since the disparate power in the signal does not affect the performance while nonlinear receivers take into account the power of each user [13].

2.2.2 Asynchronous versus Synchronous

Linear receivers project their incoming received signal vectors onto a state space which are orthogonal to each other and therefore, the presence of interference is non-existent. Hence, there is no need for synchronization. Non-linear receivers need to detect the presence of each user and therefore synchronisation becomes essential. Asynchronous detection is still possible with nonlinear receivers but it leads to a substantial increase in complexity.

2.2.3 Linear versus Nonlinear

A major drawback of linear equalizers is their vulnerability and ineffectiveness to deep fades [15]. In other words, linear equalizers suffer when the frequency response of the frequency selective channel contains deep fades. This is not apparent in nonlinear equalizers and their performance under deep fades can also be harnessed significantly [16].

University of Hertfordshire, 2011

2.2.4   Limitations under Practical Operating Conditions

The most practical operating condition is the transmission channel itself. Linear receivers do not require prior knowledge of the channel unlike nonlinear receivers. Nonlinear receivers would normally require knowledge of the channel gains of each user. The transmission channel is never constant and varies over time; hence, determining the channel gains leads to added complexity. A significant deviation from the actual channel transfer function at any given time can seriously hamper the performance of a non-linear receiver; hence research into blind multi-user receivers [14] where close approximations to the channel transfer functions have been investigated.

2.3   Multi-user Detectors for SISO Systems

Detection of signals at the receive end used to normally be in the 'single-user' scenario. In the advent of the advantages of multi-user transmission, i.e. Figure 2-2, a need for an adequate multi-user detection has also arisen. The current 'matched filter' detectors utilised for the existing single user systems are not sufficient on their own to detect multi-user signals; this is due to the presence of Multiple Access Interference (MAI) within the multi-user signals. As the number of active users increases, the MAI term disrupts the BER of the detected signal when using the conventional matched filters. The MAI is filtered out by the matched filters and treated as noise. This MAI still possesses parts of the signal and therefore, useful information when determining the value of the actual signal is being thrown away.

University of Hertfordshire, 2011
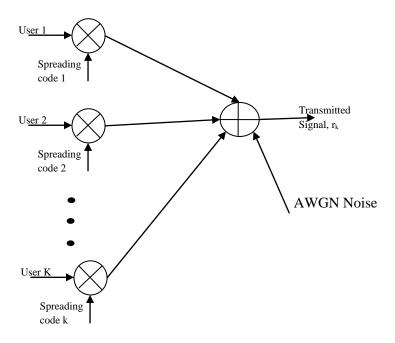
Figure 2-2:   A Typical Multi-user CDMA Transmitter

Referring to MUD receiver classification tree above, i.e. Figure 2-1, there are 2 major forms of sub-optimal detectors. It is important to understand the key concepts, advantages and disadvantages of the systems in order to facilitate and decide the choice of detectors to be utilized. The most common detector configurations have been investigated for both the linear and non-linear scenarios.

2.3.1 Linear Detectors

The aim of linear multi-user detectors is to perform a linear operation on the matched filter outputs, aimed at producing a refined set of decision statistics with reduced MAI seen by each user, hence become near-far resistant. The two most common are described below.

University of Hertfordshire, 2011

2.3.1.1 The De-correlating Detector

It performs a linear transformation on the set of matched filter outputs from the first stage. As the name implies, it de-correlates (i.e. process that is used to reduce the auto-correlation within a signal or cross-correlation within a set of signals, while preserving other aspects of the signal) the user signals so as to isolate the user from one another. This process is achieved by computing the PN code waveform cross correlation values and storing these in a KxK matrix (reason it is known to have a K^2 complexity). The vector of the matched filter outputs are then multiplied by the inverse of this matrix [19]. The receiver is insensitive to the near-far effect as prior knowledge of the channel parameters is not required. The receiver produces a significant performance when compared to the conventional matched filter receiver although it suffers from a major disadvantage of enhancing the noise statistics as a result of the de-correlation process. Due to this disadvantage, it has been neglected in the context of linear detectors examined.

2.3.1.2 The MMSE Detector

This operates similarly to the de-correlating detector with respect to applying a linear transformation to the matched filter outputs at the first stage. The function of the detector is to minimise the average squared error between the actual data and the detected data, i.e. output from the matched filter. This attribute makes the MMSE detector favourable when compared to the de-correlating detector due to the simple reason that it does not amplify noise. The drawback incurred because of this attribute, is a need to possess knowledge of the channel parameters [70]. It has been shown [12] that the MMSE displays a better bit error rate, BER compared to the de-correlator but at its limit; i.e. when the noise level drops to zero, its performance approaches that of the de-correlator. It has also been shown to possess a slightly lower near-far resistance [20], [21].

University of Hertfordshire, 2011

Another useful linear detector which is widely used is the **Least Squares** detector; this is similar to the MMSE with respect to minimising the sum of the squared error. The error referred to corresponds to the subtraction of the detected signal from the original signal [4].

2.3.2   MUD Algorithm for the Linear Detectors

The following is the derivation of the utilised equations.

- Using the one-shot demodulation assumption: the ith data symbol of the K users is given by the vector, $r(i)$ whose k^{th} component is the output of a filter matched to s_k in the interval written as:

$$r_k(i) = \int_{iT}^{(i+1)T} s_k(t - iT)r(t)dt, \qquad k = 1, 2, \dots K \qquad (2.1)$$

- Assuming all N chip samples at the ith symbol instance, the received discrete-time signal can be written in vector form as:

$$r(i) = SAb(i) + n(i) \qquad (2.2)$$

- Since the discrete-time signal, $r_k(i)$ is statistically invariant to the choice of symbol interval, i; the indices can be removed without losing their generality. Hence in vector form, Equation (2.2) becomes:

University of Hertfordshire, 2011

$$r = S\theta + n \qquad \text{where } \theta = Ab \qquad\qquad (2.3)$$

S is an N by K matrix that holds the signature sequences of all the K users and θ holds the product of the transmitted bits and their corresponding amplitudes. Using [27] and (2.3), a general equation representing linear multi-user detection can be defined below as:

$$\hat{\theta} = Cr = CS\theta + Cn \qquad\qquad (2.4)$$

For the kth user case:

$$\hat{\theta}_k = C_k s_k \theta_k + \sum_{j \neq k}^{K} C_k s_k \theta j + (Cn)_k \qquad\qquad (2.5)$$

where the filter, C_k is used to obtain estimates $\hat{\theta}_k$ for the kth user from the received signal.

The equation also shows the contribution of ambient noise and the presence of MAI within the signal. The filter C_k corresponds to the transfer function of the linear detector. The following are the derivations of $\hat{\theta}_k$ for the three detectors examined; matched filter, least squares and MMSE multi-user detectors.

University of Hertfordshire, 2011

$$\hat{\theta}_{MF} = S^T r$$

$$\hat{\theta}_{LS} = (S^T S)^{-1} S^T r \qquad\qquad (2.6)$$

$$\hat{\theta}_{MMSE} = [SA^2 S^T + \sigma 2I]^{-1} SAr$$

where S represents the user spreading sequences

2.3.3   Non-Linear Detectors

In the same manner as linear detectors, nonlinear multi-user detectors perform a nonlinear operation on the matched filter outputs. The detectors to have undergone the most advancement in recent years have been investigated. A brief explanation of their basic principles is described below while a more comprehensive approach is considered in Chapter 3.

2.3.3.1 Successive Interference Cancellation (SIC)

The algorithm detects the strongest user first, subtracts it from received signal, and then detects the next strongest, etc. It can behave in two manners. Firstly, it can subtract the soft information from received signal; leads to little or non-existent error propagation but acquires an accumulating noise effect for weak users. Secondly, it can subtract hard information from received signal leading to little or no noise accumulation but possible error propagation. Successive interference cancellation could be done in a circular manner to improve the performance at the expense of low convergence and thus high complexity. MAI is reduced and near/far problem increased. Cancelling the strongest signal has the most benefit and is the most reliable cancellation [22]. Therefore being the most reliable

15

cancellation, the SIC algorithm would mainly suffer from error propagation. It also requires channel estimates at the receiver [22]. Another variation of this interference cancellation detector is the parallel interference cancellation, PIC.

2.3.3.2 Parallel Interference Cancellation (PIC)

Similar to its predecessor, the PIC detector also involves subtracting the interference of the other users. As the name implies; unlike the serial subtraction in SIC, the PIC detector cancels the estimates of the MAI from the outputs of the matched filters in a parallel manner (i.e. simultaneously). Its performance depends heavily on the initial signal estimates and it also requires channel estimates at the receiver. It performs better than SIC when all of the users are received with equal strength (e.g. under power control) [23].

2.3.3.3 Decision Feedback Equalizer (DFE)

Decision feedback equalizer (DFE) is a very popular nonlinear equalization scheme. In most cases, it is a combination of a linear equalizer and a nonlinear decision part, both parts can be implemented with different algorithms. The objective of the DFE is to incorporate both a feed-forward FIR filter as well as a feedback filter to minimize the residual inter-symbol interference, ISI. In multi-gigabit systems, the DFE is very hard to implement due to the need to resolve the decisions within picoseconds in the feedback path. DFE outperforms linear detectors in terms of throughput but the major drawback involved comprises mainly of the complexity of its deployment and some error propagation issues [24].

This project comprises the combination of a different number of MUD techniques. Therefore, a proper dissemination of each technique is required.

2.4   Simulation of Linear Detectors

The modern technological world of today makes it possible to understand and research wireless systems using a number of software. The software chosen to simulate this project is "MATLAB" due to its broad use within the industry. It is user-friendly software that has been specifically designed to allow engineers and scientist to model everyday occurrences to the best approximation possible. The project objective is very direct but the implementation is very broad as it involves the integration of a numerous number of communication systems. The main stages utilised within this project are listed below:

- Design and simulate linear multi-user detectors for single carrier CDMA
- Combine the chosen linear detector with a PIC receiver
- Extend it using the MIMO architecture
- Improve total performance by incorporating the Sphere Decoding Algorithm

The simulations below summarise the initial stage within the project. It involved a comparison between the conventional matched filter detector and the two significant industrial linear detectors; Least Squares detector and the MMSE detector. The desired choice of MMSE and PIC has been combined and their performance evaluated

The following were derived using MATLAB as a means for comparison between the following three detectors; conventional matched filter, least squares detector and the MMSE detector.

- Bit Error Rate versus The number of Users, as shown in Figure 2-3.
- Bit Error Rate versus Signal to Noise Ratio, as shown in Figures 2-4 & 2-5 with different number of users.

University of Hertfordshire, 2011
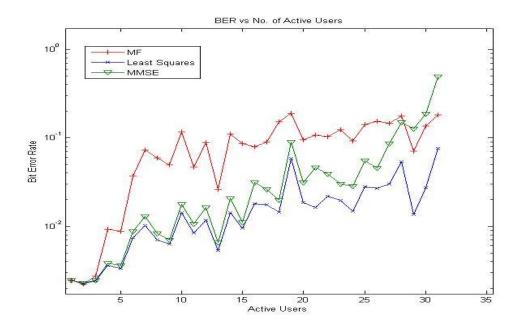
Figure 2-3:   BER vs. No. of Users
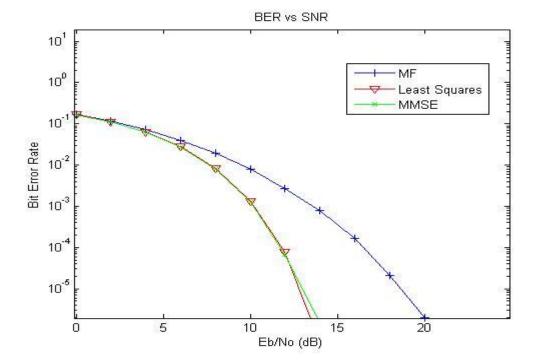
Figure 2-4:   BER vs. SNR with 5 users

University of Hertfordshire, 2011
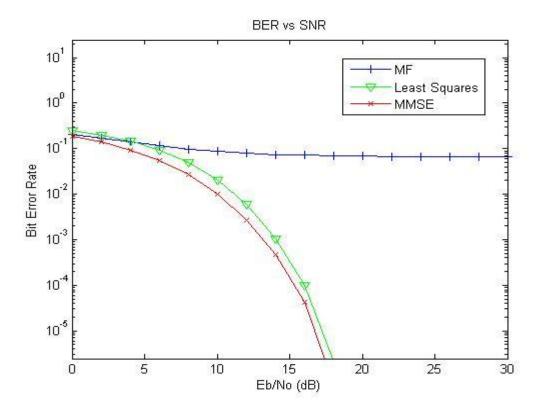
Figure 2-5:   BER vs. SNR with 10 users

The results in Figures 2-3, 2-4 and 2-5 clearly describe the advantages of utilising the MMSE detector compared to the conventional matched filter detector and the least squares detector. It can be seen from these figures that the MMSE gives a better SNR and also provides better BER for an increasing number of users. The figures also explain the need for multi-user detection as the conventional matched filter deteriorates as the number of active users increase. In Figure 2-5, a high roll off is noticed with regards to the MF estimate when compared to the previous MF estimates in Figure 2-4.

University of Hertfordshire, 2011

2.5   Simulation of Non-Linear Receiver Combinations

The initial simulations proved that the MMSE offers significant improvement when compared to its other counterparts discussed above. However, the ever increasing demand for higher data rates calls for even higher improvements in the BER. This was envisaged by combining the MMSE algorithm with the PIC algorithm which has also been evaluated in previous literature such as [12]. A receiver utilising this configuration was analysed up to an n-stage system. It is easily seen in Figure 2-6 that the BER values improve with increasing PIC stages. However, it is worth to note that the complexity of the PIC system increases with the number of stages which leads to a trade off during system design. Figure 2-6 also shows that the addition of the MMSE stage to the PIC algorithm yields a better BER value. This addition however increased the simulation time compared to the PIC stand-alone simulations.
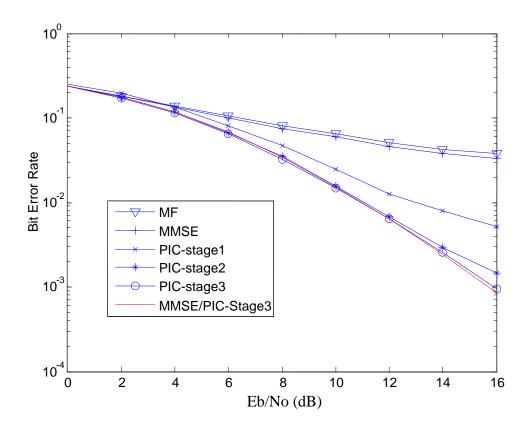
Figure 2-6:   BER for n-stage PIC detector

University of Hertfordshire, 2011

It would be worth to note again that as $\sigma \to 0$, i.e. noiseless wireless channel; the MMSE/PIC approximates to a simple PIC algorithm simply due to the reasoning that its MMSE counterpart approximates to a matched filter.

2.6   Summary

A few multi-user detectors have been examined above where the MMSE outperforms other linear detectors and the *n-stage* PIC surpassing the SIC. The evaluated detectors were studied as they also take the correlative structure of MAI found in CDMA into account during the detection process. A conventional linear detector shows relatively poor performance when the number of users is large and also since in effect it is essentially a bank of matched filters, the limitations in the presence of noise and multipath are making its use redundant in complex modern day detectors. The MMSE detector can be viewed as an upgrade of the de-correlating detector. Hence, its selection as one of the linear detectors examined with respect to combination with other types of detectors as seen in the latter chapters.

It is also seen that SIC and PIC algorithms outperform their MF and MMSE counterparts. The main attraction of the MMSE/PIC detector is the manner at which the interference caused by the incident system noise is used to improve the signal reception.

University of Hertfordshire, 2011

3   The 'MIMO' Technology

3.1   Introduction

The term 'MIMO' is used to describe systems that employ the use of multiple antennas at both transmitter and the receiver so as to improve performance by achieving higher bit error rates. It is one of the several forms of the smart antenna [5] technology. It is one of the major developments in the third generation wireless communication system and is internationally researched. The signals are transmitted in multiple paths and therefore introduce spatial diversity on the data stream in the channel. It is unlikely that all the paths would encounter severe fading at the same time which allows the MIMO scheme to improve the signal liability in a natural wireless environment.

MIMO systems [6] have become attractive trends for broadband wireless communications such as wireless LAN (IEEE 802.11n), WCDMA and WiMAX (IEEE 802.16); this is partly due to the significant increase in data throughput and link range without the need to either increase the transmit power or the system bandwidth.

3.2   Overview of MIMO Wireless Systems

Different streams of data are sent into the channel by the multiple transmit antennas at the transmitter. The transmitted streams are subjected to a communication channel made up by the matrix representation formed via the presence of multiple antennas at both transmit and receive ends [6]. The receiver then decodes the multiple received signal vector to extract the original data stream.

University of Hertfordshire, 2011

The overall capacity and performance of a MIMO system is dictated by the design objective in question. Depending on the required scenario, MIMO systems are normally employed using one or a combination of the following techniques.

3.2.1 MIMO with Pre-Coding

Pre-coding is an adapted beam-forming [7] method used to support multi-layer transmission in MIMO radio systems. Beam-forming is a process where the same signal is transmitted from each antenna with adequate weighting of its associated power and phase in order to maximise the signal power at the receiver antenna. This particular set-up is affected by factors such as line of sight and positioning; hence, it needs to be adapted for the MIMO scenario.

MIMO receivers have multiple antennas and therefore single layer beam-forming is not sufficient to simultaneously maximise the received signal levels at all the receive antennas. To achieve this, pre-coding is used to handle this multi-layer level structure of the MIMO configuration to enhance the overall performance of the system. In such systems where pre-coding is used, multiple streams of the intended transmission signal(s) are modulated into the channel with independent weighting per each receive antenna. This would yield the required increase in data throughput at the receiver output. Pre-coding requires prior knowledge of the channel state information, CSI at the transmitter to be successfully deployed.

3.2.2 MIMO with Spatial Multiplexing

A high data rate signal is normally transmitted by splitting it into multiple lower rate data streams. Each stream is then transmitted from a different antenna in the same frequency channel. At the receiver, these streams can be separated into parallel channels as long as they

arrive at the receiver antenna with different spatial signatures. This method of multiplexing can be implemented with or without CSI knowledge.

3.2.3   MIMO with Diversity Coding

In a typical MIMO communication scenario where the CSI is not known, diversity coding techniques are employed to enhance system performance. A single stream is transmitted from each antenna using various coding techniques such as space-time coding which employ partial or full orthogonal coding. Due to the nature of modern day communication wireless systems, a path from transmitter to receiver via a line of sight is normally rare hence diversity schemes employ means by which the multiple paths created by the interaction of the transmitted signal and the environment (i.e. buildings, trees, mountains etc.) can be harnessed to achieve the best assumption to the transmitted stream as possible. Space time coding is normally employed to harness the signal seen at the receiver. The transmitted signal normally undergoes phase shifts, time delays and various degradations due to the multi-path scenario. No CSI knowledge is required at the receiver. Different diversity coding schemes exist but the final choice of scheme or MIMO configuration is normally dependent on the requirements of the system to be designed. An example of a MIMO uplink system is shown in Figure 3-1.

University of Hertfordshire, 2011
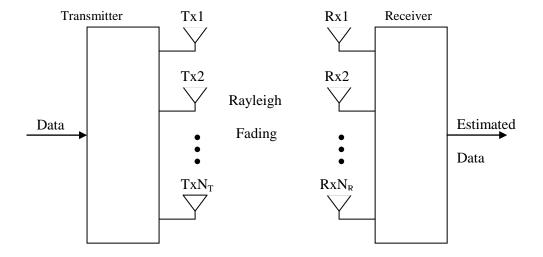
Figure 3-1:   A Typical MIMO System

To further evaluate the MIMO system, a linear representation of its associated signals is required. Assuming a system comprising N transmit and M receive antennas where x_n represents the transmitted signal, h_{mn} is the relevant entry in the channel matrix, H and n_n is the noise; the received signal y_m is represented as follows:

$$y_m = \sum_{n=1}^{N} h_{mn} x_n + n_n \quad m = 1,2,...M \tag{3.1}$$

The multiple transmit and receive antennas create channel coefficients that can be realised in the form of an M x N channel matrix shown below.

University of Hertfordshire, 2011

$$H = \begin{bmatrix} h_{11} & h_{12} & ... & h_{1N} \\ h_{21} & h_{22} & ... & h_{2N} \\ \vdots & \vdots & \ddots & \vdots \\ h_{M1} & h_{M2} & ... & h_{MN} \end{bmatrix} \qquad (3.2)$$

Therefore; at any given time, t, the received signal can be expressed as shown below.

$$y(t) = Hx(t) + n(t) \qquad (3.3)$$

where $n(t)$ represents the noise with a variance of σ^2. A means of understanding the advantages of MIMO systems is by their system throughput; i.e. capacity.

3.3 Capacity of a MIMO System

The equations for MIMO capacities have been derived, documented and included in [7]. These have been derived under a number of assumptions including:

- channel knowledge at the receiver
- additive white Gaussian noise and total transmitted power remain constant irrespective of the number of transmit antennas.
- narrowband Rayleigh channel exists during the data burst

Under the above assumptions; the overall channel capacity is given by using the following equations [8], [9], [10], [11].

$$C = \log_2 \det\left[I_m + (\rho/n)HH^H\right] \text{ b/s/Hz} \tag{3.4}$$

$$C = \log_2 \det\left[I_m + \frac{\rho}{n}R\right] \text{ b/s/Hz} \tag{3.5}$$

where C represents system capacity, I_m represents an identity matrix, ρ represents the average SNR exhibited at each receiving antenna and R represents the normalised channel correlation matrix.

Using the single value decomposition theory [11], MIMO system capacities can be visualised via a "water filling" algorithm [8], [11]. This leads to the popular equation below.

$$C = \sum_1^k \log_2 \det\left[1 + \frac{\rho}{n}\lambda_i\right] \text{ b/s/Hz} \tag{3.6}$$

where k represents the rank of the matrix and λ_i is the ith eigenmode of HH^H matrix.

This equation enables the visualisation of a MIMO channel as a number of parallel single-input single-output, SISO pipes with gains equal to their respective eigenvalues. Therefore, if the channel is known at the transmitter, the overall capacity can be increased by using only the "**good channels**" i.e. the channels that exhibit the highest gains under an unequal power distribution. This allows (3.6) to be transformed into (3.7) below.

$$C = \sum_{1}^{k} \log_2 \det\left[1 + \frac{p_i}{\sigma^2}\lambda_i\right] \text{ b/s/Hz} \qquad\qquad (3.7)$$

where p_i is the power in the ith pipe.

This value can be determined using the water-filling solution discussed earlier. It is worthwhile to note that the capacity realised from a single user MIMO system differs to that of multi-user systems.

3.4   MIMO Detectors

There are numerous detectors available but they are mostly a combination of linear and/or non-linear detectors. The most common detectors are ZF, MMSE, OSIC and VBLAST schemes. New technologies such as Sphere Detectors are emerging and offering Bit Error Rates closer to the ML approximation with lesser system complexity. These detectors where compared using different antenna configurations and modulation techniques. There are a lot of different configurations of MIMO but the adopted method and the assumptions made during this research are highlighted below.

3.4.1   Zero Forcing (ZF) Detector

This is one of the simplest algorithms available. It works as a standard equalizer where the inverse of the channel frequency response is applied to the received signal. This theoretically sounds efficient but in practical situations, it is very susceptible to noise as the

inverse of the received noise is also applied to the signal since the channel response includes noise as depicted in (3.3). Therefore, the ZF algorithm is very good for noiseless channels as it would successfully eliminate all inter-symbol interference, ISI but impractical for a noisy channel as it would amplify the noise experienced at the receiver [12].

Obviously, in order to utilise this algorithm; the channel knowledge is required at the receiver which adds to system complexity. Therefore, with respect to MIMO systems, the estimate, $\overline{y}$ of the received signal, y can be written as:

$$\overline{y}_{ZF} = (H^H H)^{-1} H^H y = H^+ y \tag{3.8}$$

where H^+ corresponds to the Moore-Penrose inverse which is essentially a pseudo-inverse of the matrix, H.

The MIMO System can be further analysed below using (3.3). It is evident that the data seen by both receivers is made up of signals from both transmit antennas. The received data seen by both receive antennas during the first time slot is y_1 and y_2 in this case where $n = m = 2$.

$$y_1 = h_{1,1} x_1 + h_{1,2} x_2 + n_1 \quad ; \qquad y_1 = [h_{1,1}, h_{1,2}] \begin{pmatrix} x_1 \\ x_2 \end{pmatrix} + n_1 \tag{3.9}$$

$$y_2 = h_{2,1} x_1 + h_{2,2} x_2 + n_2 ; \qquad y_2 = [h_{2,1}, h_{2,2}] \begin{pmatrix} x_1 \\ x_2 \end{pmatrix} + n_2 \tag{3.10}$$

University of Hertfordshire, 2011

$$y = y_1 + y_2$$

(3.11)

$$\begin{bmatrix} y_1 \\ y_2 \end{bmatrix} = \begin{bmatrix} h_{1,1} & h_{1,2} \\ h_{2,1} & h_{2,2} \end{bmatrix} \begin{bmatrix} x_1 \\ x_2 \end{bmatrix} + \begin{bmatrix} n_1 \\ n_2 \end{bmatrix}$$

x_1 : The transmitted symbol from the first antenna

x_2 : The transmitted symbol from the second antenna

y_1 : Received signal evident on the first transmitter

y_2 : Received signal evident on the second transmitter

$h_{1,1}$: Channel from the first transmit antenna to first receive antenna

$h_{1,2}$: Channel from the second transmit antenna to first receive antenna

$h_{2,1}$: Channel from the first transmit antenna to second receive antenna

$h_{2,2}$: Channel from the second transmit antenna to second receive antenna

n_1 : Noise at the first receiver

n_2 : Noise at the second receiver

The H matrix in (3.11) is the matrix whose equivalent of H^+ is given in (3.12).

$$H^+ = (H^H H)^{-1} H^H = \begin{bmatrix} \overline{h}_{1,1} & \overline{h}_{2,1} \\ \overline{h}_{1,2} & \overline{h}_{2,2} \end{bmatrix} \begin{bmatrix} h_{1,1} & h_{1,2} \\ h_{2,1} & h_{2,2} \end{bmatrix}$$

(3.12)

$$H^+ = \begin{bmatrix} h_{1,1}{}^2 + h_{2,1}{}^2 & \overline{h}_{1,1}h_{1,2} + \overline{h}_{2,1}h_{2,2} \\ \overline{h}_{1,2}h_{1,1} + \overline{h}_{2,2}h_{2,1} & h_{1,2}{}^2 + h_{2,2}{}^2 \end{bmatrix}^{-1} H^H$$

Adapting the solution for H^+ to higher order antenna configuration is more tasking and causes higher system complexity. For instance, solving for the inverse of a matrix for a *4x4* MIMO system where $n = m = 4$ can be represented below using a similar procedure as the $n = m = 2$ above.

For $H = \begin{bmatrix} h_{1,1} & h_{1,2} & h_{1,3} & h_{1,4} \\ h_{2,1} & h_{2,2} & h_{2,3} & h_{2,4} \\ h_{3,1} & h_{3,2} & h_{3,3} & h_{3,4} \\ h_{4,1} & h_{4,2} & h_{4,3} & h_{4,4} \end{bmatrix}$

(3.13)

There are now four different antenna signatures received at the receiver due to the presence of the four receive antennas as shown below.

$$y_1 = [h_{1,1} \; h_{1,2} \; h_{1,3} \; h_{1,4}] \begin{pmatrix} x_1 \\ x_2 \\ x_3 \\ x_4 \end{pmatrix} + n_1$$

$$y_2 = [h_{2,1} \ h_{2,2} \ h_{2,3} \ h_{2,4}] \begin{pmatrix} x_1 \\ x_2 \\ x_3 \\ x_4 \end{pmatrix} + n_2$$

$$(3.14)$$

$$y_3 = [h_{3,1} \ h_{3,2} \ h_{3,3} \ h_{3,4}] \begin{pmatrix} x_1 \\ x_2 \\ x_3 \\ x_4 \end{pmatrix} + n_3$$

$$y_4 = [h_{4,1} \ h_{4,2} \ h_{4,3} \ h_{4,4}] \begin{pmatrix} x_1 \\ x_2 \\ x_3 \\ x_4 \end{pmatrix} + n_4$$

Therefore:

$$y = \begin{pmatrix} y_1 \\ y_2 \\ y_3 \\ y_4 \end{pmatrix} = \begin{bmatrix} h_{1,1} & h_{1,2} & h_{1,3} & h_{1,4} \\ h_{2,1} & h_{2,2} & h_{2,3} & h_{2,4} \\ h_{3,1} & h_{3,2} & h_{3,3} & h_{3,4} \\ h_{4,1} & h_{4,2} & h_{4,3} & h_{4,4} \end{bmatrix} \begin{pmatrix} x_1 \\ x_2 \\ x_3 \\ x_4 \end{pmatrix} + n_1 \qquad (3.15)$$

$$H^+ = (H^H H)^{-1} H^H \qquad (3.16)$$

Recalling (3.13), the inverse of a *4x4* matrix is required. The values for determinant are required to calculate its inverse, the elements of the new matrix formed by H^+. The inverse of a matrix is normally realised by using co-factors. This technique adds significant and unnecessary complexity to the system for higher order of the H^+ matrix.

3.4.2   Minimum Mean Squared Error (MMSE) Detector

This is an algorithm which performs better than the ZF under noisy conditions. Although, it does not fully eliminate ISI like the ZF algorithm; it substantially reduces the total noise power experienced at the receiver [4].

$$\bar{y}_{MMSE} = (H^H H + (\sigma_n / \sigma_s)^2 I)^{-1} H^H y \tag{3.17}$$

where σ_n and σ_s represent the noise power and received signal power respectively and I represents an identity matrix. It should be noted that when $\sigma_s \gg \sigma_n$; the MMSE estimate equates to the ZF estimate. Therefore, the 2x2 and 4x4 estimates from (3.17) can be viewed as similar to their ZF counterparts with the introduction of a scaling factor.

3.4.3   Successive Interference Cancellation

The algorithm detects the strongest user first, subtracts it from received signal, and then detects the next strongest, etc. It can behave in two manners. Firstly, it can subtract the soft information from received signal; leads to little or nonexistent error propagation but acquires an accumulating noise effect for weak users. Secondly, it can subtract hard information from received signal leading to little or no noise accumulation but possible error

33

propagation. Successive interference cancellation could be done in a circular manner to improve the performance at the expense of low convergence and thus high complexity. MAI is reduced and near/far problem increased. Cancelling the strongest signal has the most benefit and is the most reliable cancellation [22]. Therefore being the most reliable cancellation, the SIC algorithm would mainly suffer from error propagation. It also requires channel estimate at the receiver [22]. Pre-filtering for general SIC systems normally adopt either a ZF or an MMSE detector. A detector using the ZF algorithm for pre-coding is examined below.

SIC systems need initial estimates to perform efficiently. These initial estimates are obtained from the output of the ZF detector. Depending on the number of MIMO antennas; estimates of the transmitted symbols x_1 and x_2 for a *2x2* scenario and x_1, x_2, x_3 and x_4 for the *4x4* scenario are obtained.

The SIC detector then takes these estimates and deducts it from the original input stream. Again the total number of iterations would depend on the number of antennas utilised. In a *2x2* scenario, only one estimate is required while in the *4x4* scenario, three estimates are required.

Using (3.8) above for a ZF detector, the estimates for a *2x2* and a *4x4* MIMO system can be expressed respectively as shown below.

$$\begin{bmatrix} \tilde{x}_1 \\ \tilde{x}_2 \end{bmatrix} = H^+ \begin{bmatrix} y_1 \\ y_2 \end{bmatrix} \qquad (3.18)$$

$$\begin{bmatrix} \tilde{x}_1 \\ \tilde{x}_2 \\ \tilde{x}_3 \\ \tilde{x}_4 \end{bmatrix} = H^+ \begin{bmatrix} y_1 \\ y_2 \\ y_3 \\ y_4 \end{bmatrix} \qquad (3.19)$$

Adopting a 2x2 MIMO system for simplicity, the incident received signal at the first receive antenna, y_1 is shown below.

$$y_1 = h_{1,1}x_1 + h_{1,2}x_2 + n_1 = [h_{1,1} \ h_{1,2}]\begin{bmatrix} x_1 \\ x_2 \end{bmatrix} + n_1 \qquad (3.20)$$

Consequently, the received signal at the second receiver corresponds to y_2 below.

$$y_2 = h_{2,1}x_1 + h_{2,2}x_2 + n_2 = [h_{2,1} \ h_{2,2}]\begin{bmatrix} x_1 \\ x_2 \end{bmatrix} + n_2 \qquad (3.21)$$

Using (3.1) where

$$y_m = \sum_{n=1}^{N} h_{mn}x_n + n_n \qquad m = 1,2,...,M$$

$$y = Hx + n \qquad (3.22)$$

As the MMSE and ZF counterparts can be viewed as significantly similar via a weighting factor, the ZF approach is adopted for simplicity purposes. Estimates of the incoming signal are decoded using the ZF algorithm by meeting the constraint below where

35

University of Hertfordshire, 2011

H^+ is a matrix inheriting the size attributes of its parent matrix, H that exhibits the relationship shown in (3.23).

$$H^H H = I \tag{3.23}$$

I is an identity matrix and using the convenient properties of an identity matrix [12], the matrix, H^+ can be written below as:

$$H^+ = (H^H H)^{-1} H^H \tag{3.24}$$

The estimates received can be visualized as depicted in (3.25) using the relationship in (3.22) to solve for the received estimates.

$$\begin{bmatrix} \bar{x}_1 \\ \bar{x}_2 \end{bmatrix} = H^+ \begin{bmatrix} y_1 \\ y_2 \end{bmatrix} \tag{3.25}$$

$$\begin{bmatrix} \bar{x}_1 \\ \bar{x}_2 \end{bmatrix} = (H^H H)^{-1} H^H \begin{bmatrix} y_1 \\ y_2 \end{bmatrix} \tag{3.26}$$

University of Hertfordshire, 2011

Assuming the first estimate to be subtracted is $\tilde{x}_2$ and given the estimates in (3.26), the received signal comprises only the remaining estimate, $\tilde{x}_1$ as shown in (3.27).

$$\begin{bmatrix} r_1 \\ r_2 \end{bmatrix} = \begin{bmatrix} h_{1,1} \\ h_{2,1} \end{bmatrix} x_1 + \begin{bmatrix} n_1 \\ n_2 \end{bmatrix}$$

(3.27)

From (3.27); it can be seen that after one iteration, the incident signal at the receiver consists of the other symbol but for cases with a higher number of transmit antennas, more iterations will suffice and the composition of the received signal will be a combination of the elements of the other transmitted signals. This can be seen from the description of the received signal after the first iteration for a *4*x*4* MIMO system.

$$\begin{bmatrix} r_1 \\ r_2 \\ r_3 \\ r_4 \end{bmatrix} = \begin{bmatrix} h_{1,1} & h_{1,2} & h_{1,3} & h_{1,4} \\ 0 & 0 & 0 & 0 \\ h_{3,1} & h_{3,2} & h_{3,3} & h_{3,4} \\ h_{4,1} & h_{4,2} & h_{4,3} & h_{4,4} \end{bmatrix} \begin{bmatrix} x_1 \\ 0 \\ x_3 \\ x_4 \end{bmatrix} + \begin{bmatrix} n_1 \\ 0 \\ n_3 \\ n_4 \end{bmatrix}$$

(3.28)

It can be seen the manner at which the new values for the H matrix change after each iteration; i.e. the corresponding *h* values are set to zero and the iteration repeats with the new value of *r* till all the transmitted symbols have been decoded.

3.4.4 Ordered Successive Interference Cancellation (OSIC) Algorithm

This is a form of non-linear equalization and is the detection algorithm utilised in this project. The major impairment in MIMO systems is Co-Antenna Interference, CAI. This impairment is readily avoided using the OSIC algorithm. This algorithm recursively detects the incoming sub-streams i.e. layers. It would initially detect the strongest layer; i.e. sub-stream with the highest SNR, and then subtracts it from the original received signal to properly eliminate the CAI. This process repeats for subsequent layers; detected on a basis of their signal strength; until all the available sub-streams / layers have been detected and subtracted from the original received signal [46].

There is a need for **ordering** when using the successive interference cancellation technique as the errors associated with earlier detected layers would continually be associated with the detection system. Hence, there is a need to initially detect layers with lower error probabilities prior to detecting other layers. The process of this ordering and in effect, the OSIC algorithm can be viewed in the three major steps described below.

3.4.4.1 Interference Cancellation

On the detection of the symbol from the i_{th} transmitter, there will be interference from $i-1$ transmitters. This interference is subtracted from the original received signal as indicated in the mathematical expression below.

$$y^{'} = y - h_1 \bar{y}_1 - ... - h_{i-1} \bar{y}_{i-1} \tag{3.29}$$

where h_i represents the respective i_{th} column within the matrix H

$\overline{y}_i$ represents estimated hard decisions of the received signal, y.

3.4.4.2 Interference Nulling

This is a very crucial technique and it is usually done using some form of linear equalization algorithm. In current systems, this is achieved using ZF or MMSE [46]. This project utilised the MMSE algorithm.

3.4.4.3 Optimal Ordering

There is a huge risk of error propagation due to the nature of the detection pattern undertaken by SIC systems. Hence the entire BER performance would be greatly hindered if sub-streams with large error probabilities are detected and subtracted from the received system at the early stages of the detection. This would cause a propagation of the acquired error throughout the rest of the detection process. Optimal ordering is used to eliminate this error propagation by allowing the row within the received signal vector with the highest post detection SNR to be detected earlier than others. Therefore, there is an optimal ordering process immediately after the occurrence of the interference nulling within the OSIC decoder.

The OSIC detection algorithm is the benchmark of layered Space Time Systems. It was first introduced by Bell Labs and widely known as BLAST [46]. A dissemination of the different types of BLAST systems is given below.

University of Hertfordshire, 2011

3.5   MIMO using BLAST Techniques

The constant demand for improved capacity, higher data rates and quality of service, QoS has led to an appreciation of the probable capacity gains possible using the MIMO systems. A lot of research has been undertaken from the advent of MIMO in the mid 90s till present. This has led to different configurations of MIMO being deployed. This project utilises one of the early, famous and well known high-rate MIMO architectures known as the Bell Labs Layered Space-Time system, BLAST [46]. This takes advantage of the multiplexing nature associated with MIMO systems.In a rich scattering environment, multiple single input single output (SISO) channels are formed. This is due to the reasoning that the fading experienced by each of the spatially multiplexed paths is independent of one another. Therefore, the capacity of the BLAST architecture would increase linearly with the number of spatial multiplexed paths formed. The BLAST system can be envisaged in different configurations. The most popular are: diagonal, **D-BLAST**; horizontal, **H-BLAST**; vertical, **V**-**BLAST**; and **TURBO-BLAST**. A typical BLAST configuration is shown in Figure 3-2.
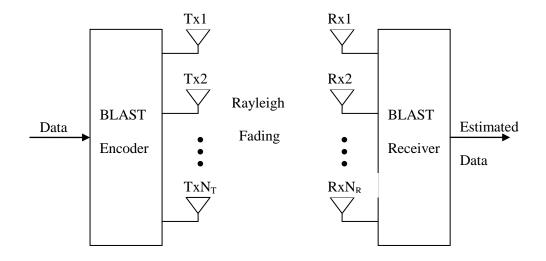
Figure 3-2:   A Typical BLAST Architecture

The initial BLAST system developed by Gerard J. Foschini in 1995 became very attractive to the telecommunications industry due to its characteristics of significantly high spectral efficiencies [42]. It significantly increases the transmission rate of the system by taking advantage of the multiplexing nature of MIMO systems. The initial BLAST architecture was the D-BLAST. It utilises multiple antenna elements at both transmit and receive ends and a diagonally layered coding structure that disperses the coded blocks across the diagonals in space-time. In a rich Rayleigh scattering environment, the capacity of this codec structure increases linearly with the number of antenna elements, which could rise to as much as 90% of the Shannon theoretical capacity limit [46]. Despite the appealing attributes offered by the D-BLAST; the realisation on chip offers significantly high complexity. As a result, different configurations of the BLAST architecture have surfaced. The main difference between these BLAST architectures is the means by which the data is transmitted. A number of these different architectures have been discussed below.

3.5.1   D-BLAST

This is the first BLAST system proposed and it has become the benchmark that subsequent BLAST architectures are built upon. Hence an elaboration on this architecture is sufficient [46]. Although, it is highly regarded within the wireless MIMO communications systems due to its high capacities offered; there is a major drawback due to the high complexity involved in its realization.

3.5.1.1 D-BLAST Transmitter

The incoming data is initially de-multiplexed from a serial data stream into a set of parallel streams. These parallel streams are then individually encoded and mapped onto

41

complex signals. The resulting symbols of these sub-streams are then mapped diagonally across the antenna arrays over time. This task is made possible courtesy of the spatial inter-leaver block as displayed in Figure 3-3.
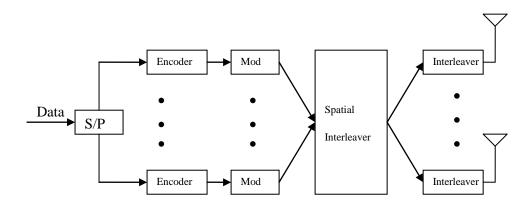
Figure 3-3:   D-BLAST Transmitter

The symbols are transmitted across the multiple antennas as described in Figure 3-4, therefore exhibiting **transmit** diversity. It would be important to highlight the reasoning that the transmitted frame might have more symbols than the number of available antennas which would therefore make the frame very long and lead to severe space time wastage [46]. This wastage is caused by the decoding nature of the receiver. The system described in Figure 3-4 describes one with four transmit antennas.

University of Hertfordshire, 2011

Symbols S1, S2, S3, S4

1	S1	S4	S3	S2	S1			
2	S2	S1	S4	S3	S2	S1		
3	S3	S2	S1	S4	S3	S2	S1	
4	S4	S3	S2	S1	S4	S3	S2	S1

Time

Figure 3-4:   D-BLAST Diagonal Layering

Figure 3-4 clearly shows the diagonal layer structure of the D-BLAST system. The corresponding wastage of space-time caused by its structure is illustrated via the unoccupied spaces in time shown in the figure.

3.5.1.2 D-BLAST Receiver

This is done by detecting the incoming received data layer by layer; i.e. it detects the first layer, discards it, detects the second layer, discards it and the cycle continues over for subsequent layers. This nature of detection contributes to space time wastage as each layer has to initially be detected first before the next. An example is shown in Figure 3-5.

The first symbol in every layer is always demodulated and detected with a great possibility of near to zero errors as it is always transmitted alone. After which the next symbol is also demodulated and detected; this symbol experiences interference from the initial layer detected. Therefore, we can call it as suffering from one interferer. The next

43

symbol is then demodulated and detected but this would suffer interference from the previous two signals; hence we can refer to it as suffering from two interferers. The process repeats for other subsequent symbols until the entire layer has been demodulated and detected [46]. After detection of the entire layer, the sub-stream associated with this layer can then be decoded. To increase the resistance against errors, the channel coding associated with the stream must be essentially long. Finally, after the entire layer has been decoded; it can be subtracted from the received data. In other words, it can then be peeled off the received data so as to expose the next layer to be detected. The process then repeats as indicated above.
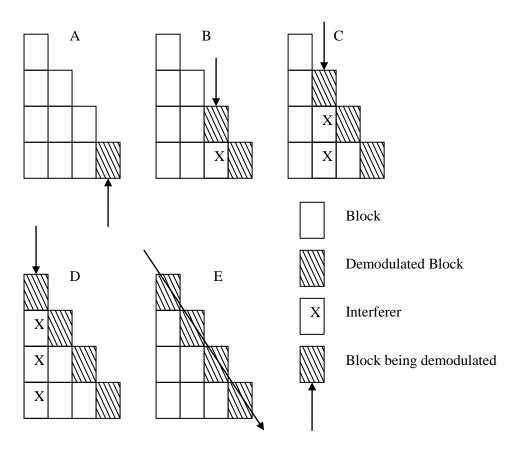
Figure 3-5:   D-BLAST Decoding Process

3.5.2   H-BLAST

This is a BLAST architecture that came into fruition during the search for an alternative to the D-BLAST architecture. It is a simpler version of D-BLAST which aims to reduce the computational complexity of the D-BLAST architecture. This new approach suffers from a drawback with respect to a loss of the transmit diversity originally provided by its predecessor. This is due to the horizontal nature by which the data is encoded. Although it suffers from this drawback, H-BLAST systems have the distinct advantage of eliminating the space-time wastage problem exhibited by the initial D-BLAST system.

The major differences between the BLAST architectures are visible from the block diagrams which show a representation of the re-arrangement of the system. An H-BLAST transmitter is shown in Figure 3-6.
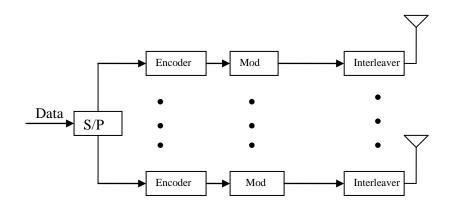
Figure 3-6:   H-BLAST Transmitter

The H-BLAST removes the Space Inter-leaver block witnessed in the D-BLAST transmitter. Each sub-stream is encoded and transmitted independently of each other. This allows the channel coding associated with a particular sub-stream to be readily available and also transmitted via the same antenna hence removing the space-time wastage problem

45

experienced using the earlier D-BLAST architecture. The decoder can be a conventional one dimensional system as the detected streams emanate from the same antenna.

3.5.3   V-BLAST Architecture

The data stream is split into multiple sub-streams and an array of antennas is used to transmit the parallel sub-streams. All the sub-streams are transmitted in the same frequency band which allows the spectrum to be used very efficiently. The V-BLAST is similar to the H-BLAST in every respect except for the type of encoding deployed [46]. This receiver has been chosen to be the focal receiver to be utilised within this project due to its lower complexity deployment compared to the other forms of BLAST architectures. A proper dissemination of the VBLAST architecture is provided in Chapter 4.

3.5.4   Turbo-BLAST Architecture

This is another derivative of the D-BLAST technique aimed at reducing its complexity. This version is exactly the same as the D-BLAST with respect to the transmitter structure but differs with respect to the encoding utilised. A special set of codes have been used to harness the high spectral capacity of the D-BLAST system without the excessive space-time wastage involved. However, there is a higher increase in the system complexity which defeats the whole objective of achieving a simpler approximate to the D-BLAST system.

3.5.5   BLAST Receivers

The main attraction of using BLAST architectures is their lower receiver complexity when compared to other MIMO systems such as those using Space Time Trellis Codes whose complexity increases exponentially with the number of transmit antennas involved. This makes the realization of these systems impractical, hence the advantage of BLAST architectures [43]. The different BLAST receivers also vary from each other with respect to the degree of complexity involved in deploying them. The best available detection method for optimal performance is the Maximum Likelihood, (ML) approach but this method suffers from a great deal of complexity and therefore leads to the use of sub-optimal approaches. These mostly comprise of linear equalization techniques such as those discussed in the previous chapter above. In this new age, a new technique has evolved known as **Sphere Decoding** [74]. This technique approaches the optimal performance with a much lower complexity when compared to the techniques discussed above. This algorithm is discussed in Chapter 5.

3.6   Simulations and Results

Assuming there is an *m*x*m* MIMO channel with a data transmission sequence, $x = [x_1, x_2, x_3, x_4, ..., x_n]$, the data is normally transmitted sequentially in a single antenna scenario and would require 'n' data time slots to transmit the data stream. In the case of the '*m*x*m* MIMO detector where there are 'm' antennas; the data can be transmitted at 'm' times the current data rate for normal transmission. This happens because 'm' symbols can now be sent in each timeslot. For example, in a *2*x*2* case, x_1, x_2 are sent from both transmit antennas in the first timeslot with x_3, x_4 are sent in the second timeslot and so on; hence, data rate is

doubled. In the *4x4* MIMO case, data rate is quadrupled as four symbols are sent in each timeslot. The other major assumptions applied are:

- the channel experiences flat Rayleigh fading
- the channel matrix, H from (3.2) is known at the receiver

3.6.1 Capacity of a MIMO System

The capacity derived above in (3.7) which was obtained using the single value decomposition theory [41] and simulated for different combinations of transmitters and receivers. A trend is immediately recognised with respect to an observed increase in capacity with an increasing number of receive antennas as depicted in Figure 3-7.
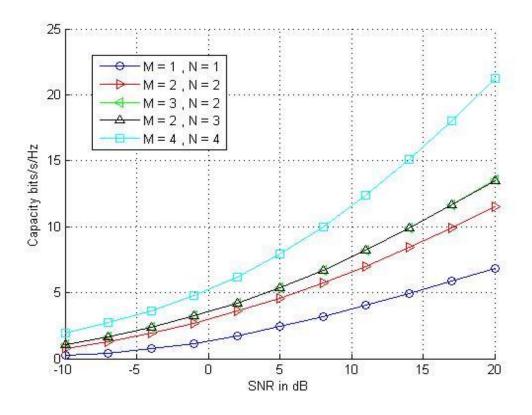
Figure 3-7:   Capacities of different MIMO Configurations

University of Hertfordshire, 2011

3.6.2 Implementation Using Different Receiver Configurations

A combination of ZF, MMSE and OSIC have been studied. The receiver combinations tested are ZF, MMSE, ZF-OSIC and MMSE-OSIC. A test message signal comprising of $n = 1x10^5$ bits transmitted through a Flat Rayleigh fading channel. The transmitted modulated signal was split into the appropriate number of streams required for the test antennas required. For instance; for a 2x2 system, the signal would be split into two independent data streams and a 4x4 system would require 4 streams etc. Figures 3-8 and 3-9 represent the BER performance of a 2x2 and 4x4 system respectively, for different receiver combinations.
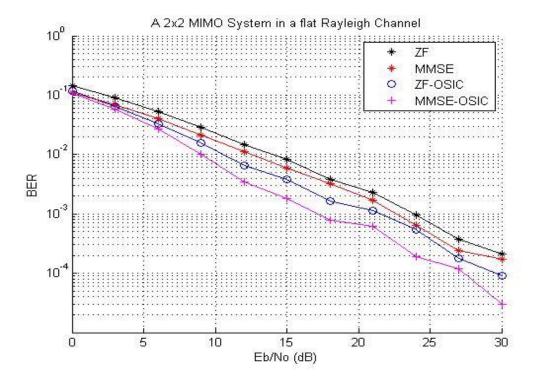
Figure 3-8:   2x2 MIMO with different Receive Architectures

University of Hertfordshire, 2011

The incoming QPSK data signal would encounter an open-loop spatial-multiplexing system [7], [10] which refers to an assumption of 'perfect channel knowledge at the receiver without the need for any feedback to the transmitting device.
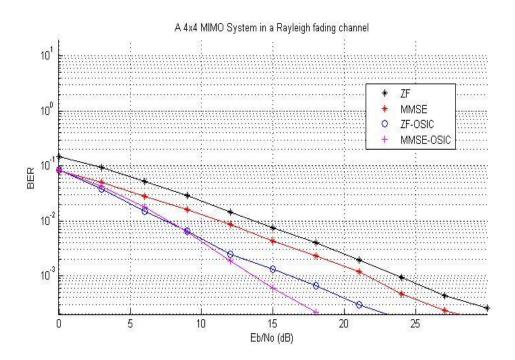
Figure 3-9:   4x4 MIMO with different Receive Architectures

A detector based on the maximum likelihood algorithm is used as a means of comparing the performance margins exhibited by each receive detector combination for a 4x4 system as shown in Figure 3-10. The transmitted signal is assumed to have a zero phase offset and Gray-scale coding is utilised at the transmitter. No spatial coding was utilised.
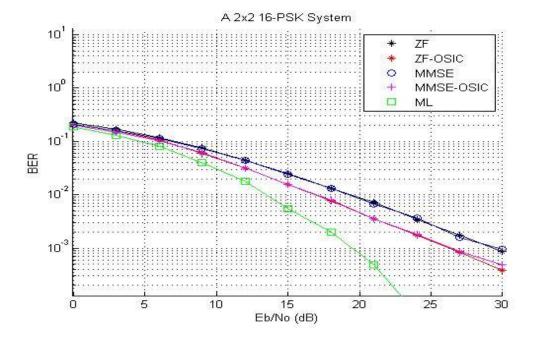
Figure 3-10:   A 2x2 MIMO System with 16-PSK modulation

3.6.3   Using different modulation schemes

The initial MIMO system was implemented using the simple QPSK digital modulation scheme. There is a need to understand the effects of different modulation schemes with the MIMO system. The system was compared using the most common modulation schemes such as BPSK, QPSK, 16-PSK and 16-QAM for a ZF receiver shown in Figure 3-11.
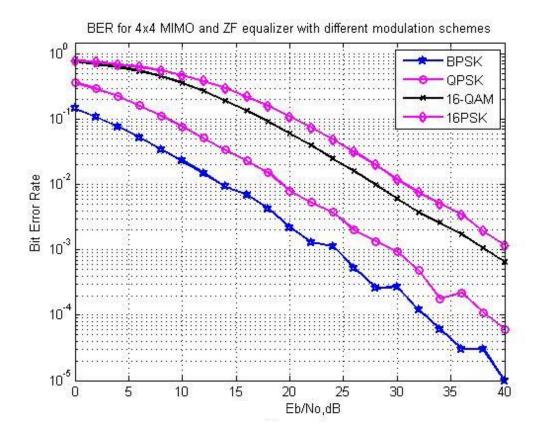
Figure 3-11:   A 4x4 MIMO with different Modulation Schemes

3.7   Summary and Analysis

The capacity of a typical MIMO system increases accordingly with an increase in the total number of antennas as shown in Figure 3-3. It can also be noticed that the capacity of an NxM MIMO system is the same as an MxN MIMO system.

The addition of SIC to both the ZF and MMSE MIMO receivers provides slight improvements to the estimated BER values but this slight improvement becomes a very substantial one when ordering is implemented with SIC as shown in Figures 3-8 & 3-9. It can also be noted as seen in Figure 3-10 where 16-PSK is utilised, the performance BER plots of MMSE-OSIC to ZF-OSIC are now similar though MMSE-OSIC still exhibits better BER

52

rates. An ML decoder is also included in Figure 3-10 to show the achievable BER rates possible using an optimal decoder that requires a much higher computational complexity.

The choice of modulation scheme depends on the scenario with respect to the factors of transmission required. For instance, 16PSK and 16QAM transmit more symbols than QPSK and BPSK. A 2x2 MIMO System was investigated as shown in Figure 3-11 with receiver architecture based on the simple ZF detector. As expected, due to increasing the total number of transmitted symbols per second, there would be an increase in the total number of errors and therefore the need to operate at a higher SNR values. The need to operate at higher SNRs for higher order modulation is also shown in Figure 3-11.

This chapter should have provided a concise understanding of a typical MIMO system. Modern day systems adopt a multi-user scenario when compared to the single user systems adopted above. The current demand for increased data rates leads to the industry utilising techniques such as OFDM; as seen in WLANs, and CDMA to further utilise the capabilities of MIMO. The next chapter looks at integrating MIMO with receive architectures based on multi-user algorithms.

4 Multi-user Detection and MIMO

4.1 Introduction

As discussed in Chapter 3, this project utilises one of the early, famous and well known high-rate MIMO architectures known as the Bell Labs Layered Space-Time system, BLAST [32]. Due to the endless demand for higher data rates for current and future systems, MIMO has proven to be a promising candidate to meet these demands through the increased capacity it offers over its SISO counterpart. Current and future systems normally operate using multi-user algorithms to meet the demand for the growing number of active users and the limited resources [22]. Multi-user systems combined with a MIMO configuration theoretically should provide higher data rates and this is investigated in this chapter.

A Multi-user MIMO (MU-MIMO) system generally comprises multiple users and a base station; which could be for both uplink and/or downlink, as shown in Figure 4-1 below.
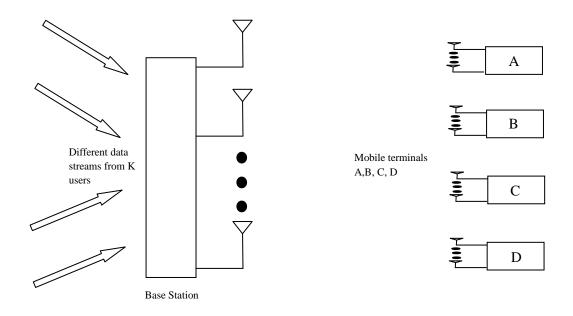
Figure 4-1:   A Multi-user MIMO uplink/downlink system

University of Hertfordshire, 2011

An example of an MU-MIMO system can be witnessed in the MIMO **broadcast channel** [12]; this basically refers to the downlink portion of MIMO systems. The downlink involves the base station sending different streams of data to multiple users as depicted in Figure 4-1. Conversely, the MIMO uplink system operates with the base station receiving different streams of data from multiple users. Research on MU-MIMO has been developing promising results with respect to performance and complexity issues since it significantly improves overall data rates without the need for extra bandwidth or increased transmit power. This attribute of MIMO is witnessed due to the higher number of bits been transmitted using the same radio resources, i.e. higher spectral efficiency [46]. MU-MIMO has been tipped as a fore-runner for current and future 3GPP LTE trends, IEEE 802.11 standards, 4G and WiMaX [35].

MIMO systems are offering large capacities with greater spectral efficiency when compared to their predecessors within the telecommunications sector. For instance, the mobile communications industry continually searches for systems to improve the capacities and throughput it currently offers due to the ever increasing consumer demand. This has led to the increased amount of research being conducted using multiple users. This development coupled with MIMO systems has become a worldwide research area aimed at increasing the overall capacity of mobile and telecommunication networks.

This chapter gives a description of a multi-user V-BLAST detection algorithm, multi-user MIMO and its combination with CDMA and OFDM systems. It further analyses the combination of these important telecommunication technologies with MIMO systems by investigating the overall BER performance of the system.

4.2   A V-BLAST MIMO Model

Vertical Blast or V-BLAST [46] is a simpler version of its predecessor, D-BLAST discussed in Chapter 3. The deployment of D-BLAST is known to have a high computational

complexity and hence a better alternative in the form of V-BLAST was deployed. MIMO using V-BLAST (i.e. spatial multiplexing) is generically referred as a **MATRIX B MIMO** design [37].

4.2.1   V-BLAST Transmitter

The incoming data stream to be transmitted is normally split into separate sub-streams where each sub-stream experiences independent encoding algorithms before being directed towards the input of a transmitting antenna. This form of layering when compared to the diagonal nature of D-BLAST is horizontal in nature which simply implies that the constituent symbols of ONE of the sub-streams are all evident on and transmitted using the SAME antenna. This form of layering would almost certainly remove the space wastage problem realised by the D-BLAST detector though it already gives an immediate drawback in the loss of transmit diversity normally exhibited by the D-BLAST receiver since the symbols of every subsequent sub-stream are not spread across all the transmit antennas. The transmitted symbol array can be envisaged as shown below.

$$s = [s_{1k}, s_{2k}, ...s_{N_T k}]^T \tag{4.1}$$

where s is the transmitted vector at any time instant, T

   s_{ik} is the kth symbol of antenna sub-stream i for $i = 1:N_T$.

4.2.2   V-BLAST Receiver

The nature of the V-BLAST layering is such that the symbols are transmitted in a vector manner with each incident vector comprising of a symbol from each sub-stream. In systems where a form of channel coding is utilised, the received symbols need to be stored in a data buffer until the adequate block size required for correct demodulation has been received. V-BLAST requires a detector to approximate the initial incident transmitted arrays before final signal detection.

Two main linear decoders are utilised in modern day systems depending on the performance requirement of the system. The Zero Forcing, ZF and Minimum Mean Squared Error, MMSE detectors are commonly used and they operate as discussed in the previous chapter above. The channel transfer characteristic for both detectors is as shown below.

$$H_{ZF} = \sqrt{N_T/E_S} * H^+ \tag{4.2}$$

$$H_{MMSE} = \sqrt{N_T/E_S} * (H^H H + N_T/\rho * I_{N_T})^{-1} * H^H \tag{4.3}$$

where H^+ represents the Moore-Penrose pseudo inverse of H

H^H represents the Hermitian transpose matrix of H

N_T represents the total number of transmit antennas

ρ is a weighting constant chosen dependent on the channel noise statistic

E_S represents the transmitted signal energy

The linear decoders behave differently when utilised as the nulling [3] algorithm for the V-BLAST system; V-BLAST utilises the non-linear O-SIC algorithm in Chapter 3 for its normal operation. The ZF contributes to the overall system noise as it tries to demodulate the

57

received signal vector by inverting the transmission channel. This is not beneficial in noisy scenarios as it would only enhance the received noise. The MMSE decoder improves on this limitation by also inverting the transmission channel but having a weighting factor allotted to compensate for the noise amplification caused by the channel inversion.

4.3   Transmitted Signal Model of V-BLAST Architecture

A high rate single data stream is converted into N_T low rate sub-streams which are encoded independently of each other and transmitted via its respective BPSK transmitters [40]. The wireless channel is assumed to be flat fading in the presence of rich Rayleigh scattering. After undergoing matched filtering and symbol rate sampling, the received signal vectors at the receiver can be written as in (4.4).

$$\mathbf{r} = [r_1, \ r_2, \ r_3, \ ... \ , r_{N_T} \ ]^{\mathrm{T}} \tag{4.4}$$

where the transmitted symbols can be described as in (4.5).

$$\mathbf{b} = [b_1, \ b_2, \ b_3, \ ..., \ b_{N_T} \ ]^{T} \tag{4.5}$$

The received signal depicted in (4.4) can be represented as in (4.6) below.

$$\mathbf{r} = H\mathbf{b} + n \qquad\qquad (4.6)$$

where the channel matrix, **H** can also be represented as columns corresponding to the N_T transmitted signals as depicted in (4.7).

$$H = [h_1,\ h_2,\ h_3,\ ...,\ h_{N_T}]^T \qquad\qquad (4.7)$$

4.4　Detection Algorithm of V-BLAST Architecture

This detection technique is based on the OSIC algorithm for signal detection initially proposed by Foschini [35]. Ordered Successive Interference Cancellation, OSIC is combined with linear nulling techniques to perform the required symbol detections. As discussed earlier, the efficiency of the system is enhanced mainly due to the ordering of the SIC technique. This ordering is based on the maximization of the post-detection signal-to-interference plus noise ratio (SINR) which is used as the reference for the ordering. The use of ZF or MMSE as the nulling process is internationally implemented hence both algorithms are utilised within this project. The following steps are followed during detection via the V-BLAST algorithm.

The index of the computational iteration is i where $1 \le i \le N_T$

- Calculation of the inverse of the channel correlation matrix:

$$\mathbf{R}(i)^{-1} = \mathrm{Re}[H^H(i)H(i)]^{-1}$$

59

- Determine the sub-stream, g whose post de-correlating SNR is the highest; this would correspond to the minimum among the first $N_T - i + 1$ diagonal entries of $\mathbf{R}(i)^{-1}$:

$$g = \arg\min[\mathbf{R}(i)_{g,g}^{-1}] \quad \text{where } g = 1, 2, ..., N_T - i + 1$$

The nulling vector $\mathbf{w}$ is the gth row of $\mathbf{R}(i)^{-1}$ and the bit estimate of the gth sub-stream is: $\quad \overline{\mathbf{b}}(i) = sign(\mathbf{w}r(i))$

- Interference cancellation is obtained by subtracting the detected signal from the received signal:

$$\mathbf{r}(i+1) = \mathbf{r}(i) - h_g\,\overline{\mathbf{b}}(i)$$

H(i) is reordered such that the gth column and the last column are then interchanged

$$H(i)' = [h_1 \ ... \ h_i \ ... \ h_{N_T} \quad h_g] = [H(i+1)h_g]$$

where *H(i+1)* is now defined as *H(i)'* with the last column h_g being deleted.

- The process repeats with i being incremented by 1 and continues until all the N_T transmitted sub-streams have been detected.

University of Hertfordshire, 2011

4.5   MIMO-CDMA

A downlink mobile telecommunications system is considered as shown in Figure 4-2. The system consists of K mobile users each possessing N_R receive antennas and a single base-station with N_T transmit antennas [58].
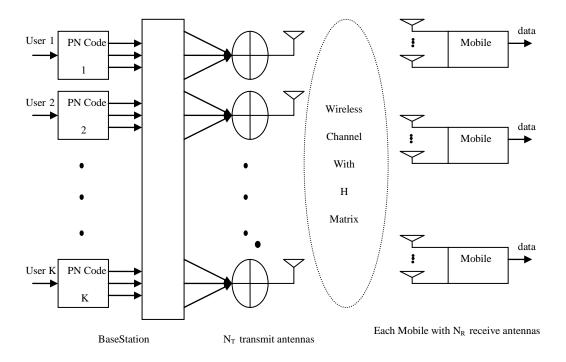
Figure 4-2:   A Typical Multi-user CDMA MIMO System

Each user is modulated using a codeword of a particular length. These are then transmitted via N_T transmit antennas leading to KN_T transmitted sub-streams within the rich scattering channel. A few assumptions have been taken into consideration. These are as follows.

- The complex fading coefficients among the antennas are uncorrelated due to the assumption that the antennas have been spaced sufficiently far apart from each other.

- Inter-symbol interference is ignored since the delay spread is small when compared to the incoming data symbol

- The time delays between antennas are independent of each other and are restricted within one symbol interval.

- The interference between frames is eliminated by inserting a blank bit interval after every M bits and selecting a received signal length of M+1 bits.

Taking the effect of multi-path into consideration, the coherently received complex baseband signal, $r_p(t)$ for a frame of M data bits at the pth (p = 1, 2, ... N_R) antenna can be represented as:

$$r_p(t) = \sum_{m=1}^{M} \sum_{n=1}^{N_T} \sum_{k=1}^{K} c_{n,p} a_{k,n} s_k(t - mT_s - \tau_{n,p}) b_{k,n}(m) + n_p(t)$$

(4.8)

where $c_{n,p}$ is the complex channel coefficient between the nth transmit antenna and the pth receive antenna

$a_{k,n}$ is the amplitude of the kth user's n^{th} sub-stream

$s_k(t)$ is the normalized PN code sequence of the kth user

T_s is the symbol interval

$\tau_{n,p}$ is the time delay of the path between the nth transmit antenna and the pth receive antenna

$b_{k,n}(m)$ is the BPSK modulated data symbol of the kth user's n^{th} sub-stream

$n_p(t)$ is the AWGN on the receive antenna p.

After passing through a chip matched filter, the discrete time complex baseband received signal for a mobile user at its pth antenna during a given symbol period; i.e. M+1, can be written as a complex N − vector as shown below:

$$\mathbf{r}_p = \mathbf{S}_p \overline{H}_p \mathbf{A} \mathbf{b} + \mathbf{n}_p \tag{4.9}$$

$$\mathbf{S}_p = [\mathbf{S}_{k,n,p}(1) \quad \mathbf{S}_{k,n,p}(2) \quad ... \quad \mathbf{S}_{k,n,p}(M)] \tag{4.10}$$

where $\mathbf{S}_p$ is the real part of the $((M+1)L)\text{x}(KMN_T)$ spreading code matrix formed from concatenating the matrices.

$$\mathbf{S}_{k,n,p}(i) = [\mathbf{s}_{1,1,p}(i) \quad ... \quad \mathbf{s}_{1,N_T,p}(i) \quad \mathbf{s}_{2,1,p}(i) \quad ... \quad \mathbf{s}_{K,N_T,p}(i)] \in \mathfrak{R}^{(M+1)L \text{x} KN_T} \tag{4.11}$$

$$\mathbf{s}_{k,n,p}(i) = \mathbf{s}_k(t - iL - \tau_{n,p}) \in \mathfrak{R}^{(M+1)L} \tag{4.12}$$

It should be noted that the matrix of (4.11) consists of columns of spreading code vectors for the transmission of the kth user data over the nth antenna. The matrix $\overline{H}_p$ is a

block diagonal of size KMN_T by KMN_T. It is made up of KM instances of the channel matrix H_p along its main diagonal.

$$\overline{H}_p = \mathbf{I}_{KM} \otimes diag(H_p \ \ldots \ H_p)$$
(4.13)

where $\otimes$ represents the Kronecker product. The matrix H_p is a complex N_T by N_T channel matrix described as follows.

$$H_p = diag(h_{1,p} \ \ h_{2,p} \ \ldots \ h_{N_T,p})$$
(4.14)

where $h_{n,p}$ represents the complex coefficient corresponding to the fading channel between the transmit antenna n and the receive antenna p. The matrix $\mathbf{A}$ is a $(KMN_T)x(MKN_T)$ diagonal matrix with its amplitudes described as shown in (4.8).

$$\mathbf{A} = \mathbf{I}_M \otimes \mathbf{a}$$
(4.15)

$$\mathbf{a} = diag(a_{1,1} \ \ldots \ a_{1,N_T} \ \ \ a_{2,1} \ \ldots \ a_{K,1} \ \ \ldots \ a_{K,N_T})$$
(4.16)

The data vector $\mathbf{b}$ is the real part of the binary data vector defined by (4.17).

$$\mathbf{b} = \begin{bmatrix} \mathbf{b}^T_{k,n}(1) & \mathbf{b}^T_{k,n}(2) & \ldots & \mathbf{b}^T_{k,n}(M) \end{bmatrix}^T$$
(4.17)

64

Assuming BPSK is the chosen digital modulation method.

$$\mathbf{b}_{k,n}(i) = [b_{1,1}(i) \ ... \ b_{1,N_T}(i) \quad b_{2,1}(i) \ ... \ b_{K,1}(i) \ ... \ \mathbf{b}_{K,N_T}(i)]^T \tag{4.18}$$

The vector $\mathbf{n_p}$ is a zero mean complex Gaussian noise (M+1)L vector with independently and identically distributed (i.i.d) components whose real and imaginary components both have a variance of $\sigma^2/2$. The power within the system is equally transmitted across the antennas. Hence each sub-stream corresponding to any user within the system possesses a transmit energy equal to $1/N_T$.

This project investigated an example of a downlink system where a single base-station is transmitting to k mobile users. When visualising the multi-user MIMO CDMA scenario, each user would only see the signal from its subsequent transmitter as shown in Figure 4.3.
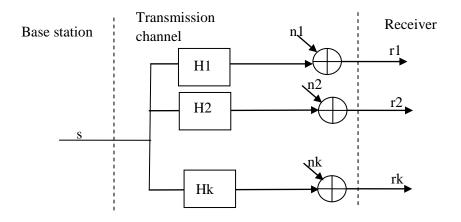
Figure 4-3: Flowchart representation of multi-user channel

University of Hertfordshire, 2011

From Figure 4-3, it can be seen that for every receive antenna, r_k; only data information from user k is meant to be witnessed but as expected in real life systems, there exists an element of noise depicted as n_k.
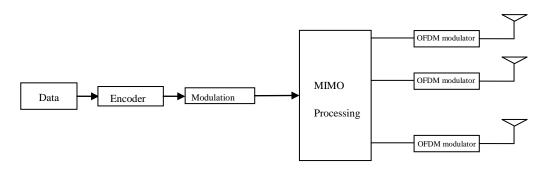
4.6   MIMO-OFDM

The advent of MIMO caused a major stir in the manner at which data rates have been perceived in the modern day telecommunications industry. As previously discussed, MIMO significantly enhances total system throughput by increased data rates between transmitter and receiver.
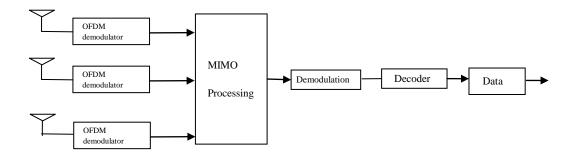
Another initiative realised by MIMO in modern telecommunication systems is its combination with another technique known as Orthogonal Frequency Division Multiplexing, OFDM. OFDM is a modulation technique which transmits data in parallel over a N sub-carriers. OFDM is readily integrated into systems as due to its use of the Fast Fourier Transform [23] principle. Therefore, system complexity is already simplified as the total number of sub-carriers will be equal to the FFT block size utilised. OFDM is a technique that harnesses the *frequency-selective* nature of the channel to enhance the transmitted signal, i.e. it converts a frequency selective channel into several flat fading channels [24]. Each sub-carrier has a designated bandwidth which is set as a fraction of the total allotted system bandwidth; this fraction is the FFT block size used in the system. Therefore, in a system with *N = 24* sub-carriers and *total system bandwidth, B,* each sub-carrier would utilize *B(Hz)/24* of the total bandwidth. In OFDM systems, a cyclic prefix is also attached to the front of every OFDM symbol to effectively eliminate the effect of inter-symbol interference from adjacent sub-carriers.

OFDM has also been recognised as a key technology in the search for improved data rates and therefore the combination of both technologies seemed inevitable. MIMO-OFDM is

66

being widely recognised and used in international standards such as in IEEE 802.11a, 802.11n, 802.16e , 3GPP & 3GPP2 for applications like WLAN, Wi-Fi, Wi-Max and internet broadcast data [29]. A simplified version of an OFDM transmission system can be seen in Figure 4-4 below.

(i)   MIMO-OFDM Transmitter

(ii)   MIMO-OFDM Receiver

Figure 4-4: A Typical MIMO-OFDM Telecommunications System

The concept of multi-user communications can be visualised from the figure above where each user has a designated transmitter.

4.6.1 A MIMO-OFDM System based loosely on the IEEE 802.11 standards

A system partially based on the IEEE 802.11 standards such as the 802.11a and 802.11g was simulated and the effect of the addition of MIMO to OFDM researched. There are some specifications generic within the 802.11a and 802.11g standards. These are shown in Table 4-1.

Specification	802.11a	802.11g
FFT Size	64	64
Used Sub-Carriers	52	48
Sub-carrier Index	[-26 to -1, +1 to +26]	[-24 to -1, +1 to +24]
FFT Sampling frequency	20MHz	20MHz
Cyclic Prefix	0.8 µs	0.8 µs
Duration of data symbol	3.2 µs	3.2 µs
Total Symbol Duration	4 µs	4 µs
Pilot Sub-carriers	4	4

Table 4-1:   Generic IEEE 802.11 specifications

The cyclic prefix is generally utilised to reduce the effect of ISI and although *52 of the 64* subcarriers are designated to be used, 4 of these are used as pilots to transmit the essential phase, frequency training and tracking. In essence, only 48 out of the 52 allotted sub-carriers are actually used to carry data.

The effect of varying different specifications such as the cyclic prefix rate and the total number of MIMO antennas was investigated for each of the 802.11 standards shown in

University of Hertfordshire, 2011

Table 4-1. Modern day systems normally allow for some wastage in bandwidth as a trade-off to increased performance. This wastage in bandwidth, known as *cyclic prefix* is used to eliminate ISI in OFDM systems despite the loss of data rate encountered from the transmission of redundant data. The cyclic prefix exhibits this property by categorically acting as a buffer between subsequent OFDM symbols.

To accommodate the desired specifications, the following parameter values were derived from the extract shown in Table 4-1.

The total number of used sub-carriers: Generally in OFDM systems, the cyclic prefix is realised via a copy of part of the signal to be attached to the OFDM frame as redundant information to battle ISI. *The number of used subcarriers* is given as 52.

Given an operating frequency of *20MHz*:

$$T_s = 3.2\mu s;$$

$$\Delta f = 1/T_s = 1/3.2\mu s = 312.5 kHz;$$

$$\Delta f_1 = \pm 312.5 kHz;$$

$$\Delta f_2 = \pm 625 kHz;$$

$$\Delta f_k = \pm k\Delta f_1;$$

$$B_{tot} = 20MHz;$$

$$C_{used} = 52;$$

$$C_{unused} = DFT_{size} - C_{used} = 64 - 52 = 12;$$

$$\Delta B = -10MHz\ ....+10MHz;$$

where T_s represents the symbol period

Δf represents the sub-carrier spacing

Δf_k represents the range of frequencies of the kth sub-carrier

B_{tot} represents the total dedicated system bandwidth

C_{used} represents the total number of used sub-carriers

C_{unused} represents the total number of unused sub-carriers

DFT_{size} is equal to the FFT size = 64

ΔB represents the range of frequencies available for operation

From the parameters above, it is visible to see although there exists an allocated frequency range, ΔB, the entire signal is not distributed along the entire available bandwidth as there are unused sub-carriers in the DFT block. In modern day systems, 4 of the unused sub-carriers in the allotted unused sub-carrier index are normally used to transmit pilot data about the OFDM frame.

The OFDM Modulator block in Figure 4-4 has been expanded into Figure 4-5 below to provide clarity on how the OFDM symbol is processed and transmitted. The manner of the addition of the cyclic prefix is also highlighted.
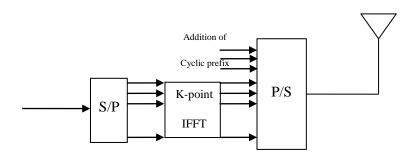
Figure 4-5:   OFDM Modulator Block of kth user

The MIMO-OFDM system being investigated consists of a system of N_t transmit and N_r receive antennas. Incoming data bits are normally modulated to form Tx^i *[n,k]* with respect to the ith transmitter; *n* represents the OFDM symbol number and *k* is the sub-carrier index. After MIMO processing, each sub-stream is orthogonally modulated onto *k* sub-carriers using a K-point Inverse Fast Fourier Transform; IFFT, and re-multiplexed with a cyclic prefix addition to form the transmitted OFDM frame. The channel between a receiver and its subsequent transmitter is assumed to be a Rayleigh fading environment with *L* taps [13]. The real and imaginary part of each tap is an independent Gaussian variable whose impulse response is represented below.

$$h(t) = \frac{1}{\sqrt{L}} \left[h_1(t-t_1) + h_2(t-t_2) + \; ... \; + h_L(t-t_L) \right] \tag{4.19}$$

The term $h_L(t-t_L)$ in (4.19) represents the channel coefficient of the Lth tap and the $\frac{1}{\sqrt{L}}$ term is used to normalise the power of the channel with respect to the total number of realised taps [13].

4.7   Simulations and Results

This chapter is based on the combination of MIMO with multi-user systems. Different sub-systems were created using the MATLAB computing software [version r2009b]. These sub-systems are then combined together to compare the BER performance of MIMO when subjected to different types of multi-user scenarios namely CDMA and OFDM. The latter has

developed more interest within the telecommunications industry of late and as such has become an interesting research area.

A *2x2* MIMO CDMA system was simulated using the same combination of receivers observed in Chapter 2 to establish the expected BER improvements exhibited by the addition of the spatial property of MIMO systems.

OFDM is a current trend in the industry because of the advantages it offers. This led to the use of MIMO as a means to increase their current effectiveness is a field that attracts a lot of interest. Hence, combination of MIMO; using spatial multiplexing, with OFDM have been investigated. The utilised linear detector is the Zero Forcing Detector for MIMO-OFDM for investigation purposes. The IEEE standards investigated were primarily 802.11a and 802.11g. 802.11n can be considered as a high throughput amendment to the 802.11 standards containing improvements over earlier 802.11 standards [29]. MIMO is currently an attractive technology when combined with OFDM due to the BER improvements offered by MIMO and the signal robustness exhibited by OFDM in a multi-path scenario makes their combination very useful in systems such as WiFi and WiMax using specifications according to the LTE, 3GPP standards.

4.7.1   Varying the number of users in a MIMO CDMA system

A 2 x 2 MIMO CDMA system was investigated. Individual user signals were simulated across $N_T = N_R = 2$. A different set of gold codes of length N = 32 was utilised for each transmit antenna and the BER performance of the multi-user MIMO-CDMA system was investigated using the detectors previously discussed in Chapter 2 for SISO CDMA have been revisited and their equivalence when subjected to a MIMO scenario have been depicted in Figure 4-6 & Figure 4-7 below where the total number of users examined were K = 5 and K = 10 respectively.

University of Hertfordshire, 2011
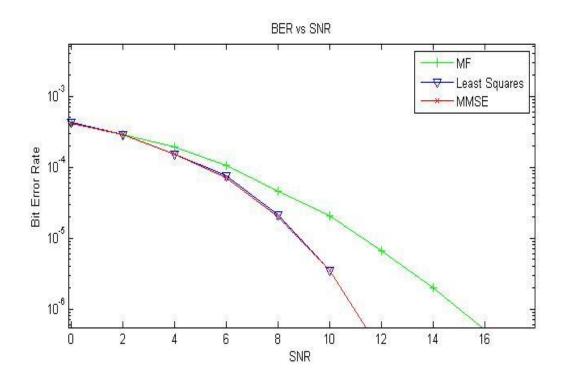
Figure 4-6:   BER for a 2x2 MIMO CDMA System for K = 5 users
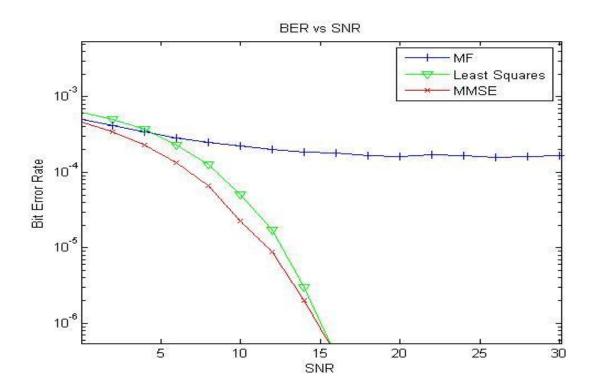
Figure 4-7:   BER for a 2x2 MIMO CDMA System for K = 10 users

University of Hertfordshire, 2011

4.7.2 Varying the Number of Antennas in a MIMO-OFDM system

The MIMO-OFDM system was simulated with $N_T = N_R$ to realise Figure 4-8 below with a total number of *10,000* OFDM frames. The results obtained in Figure 4-8 and Figure 4-9 were obtained for MIMO systems deployed using IEEE 802.11a and IEEE 802.11g respectively.
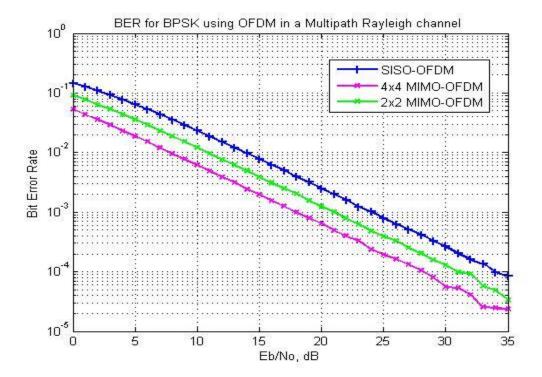
Figure 4-8: BER Performance of a MIMO-OFDM for $N_T = N_R$ = 1, 2 and 4 (802.11a)

University of Hertfordshire, 2011
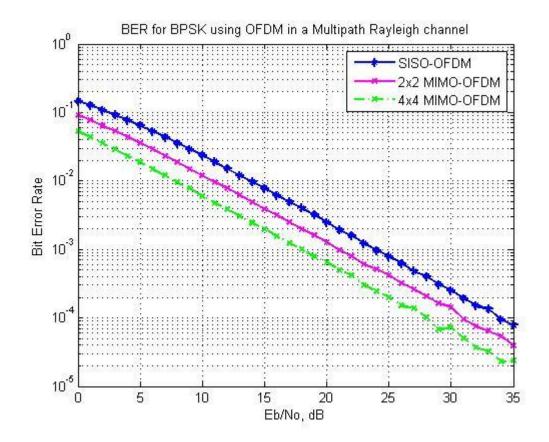
Figure 4-9: BER Performance of a MIMO-OFDM for $N_T = N_R = 1, 2$ and 4 (802.11g)

A test multi-user signal was initially modulated using BPSK modulation technique before it was split into the required number of data streams for MIMO transmission. These streams were passed through a multipath fading Rayleigh environment to be received by mobile user equipment at the receivers. The same set of conditions applied in Table 4-1 were utilised for each set of MIMO-OFDM symbol generated.

4.7.3   Varying the Guard Band Interval in MIMO-OFDM

An important factor in OFDM transmission is the cyclic prefix [67]. In essence, the effect of varying the amount of redundant information included in an OFDM symbol frame was investigated. The cyclic prefix duration utilised were grouped in rates as indicated below.

University of Hertfordshire, 2011

The achieved BER performance is shown in Figure 4-10 and Figure 4-11 below where symbol duration equals 3.2μs.

Rate I   *: 8 / 64 = 0.4 μs*

Rate II   *: 16 / 64 = 0.8 μs*

Rate III   *: 24 / 64 = 1.2 μs*
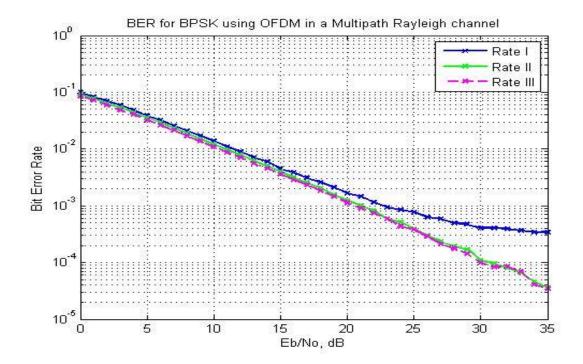
Figure 4-10: BER of a 2x2 MIMO-OFDM with different cyclic prefix lengths (802.11a)

University of Hertfordshire, 2011

BER for BPSK using OFDM in a 802.11g Multipath Rayleigh channel
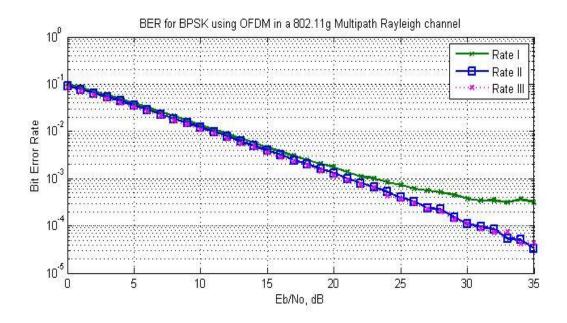
Figure 4-11: BER of a 2x2 MIMO-OFDM with different cyclic prefix lengths (802.11g)

The guard band is used to limit interference. Increasing the guard time increases the delay spread between each OFDM frame and therefore limits multipath interference between adjacent symbols. The effect of shortening the guard band would effectively reduce the delay spread but actually increase the transmitted data rate. The effect of varying this parameter was investigated for a 2x2 MIMO-OFDM system using different 802.11(a/g) standards and the results are shown in Figure 4-10 and Figure 4-11 above.

4.8   Summary and Analysis

As expected, the BER performance of the MIMO-CDMA declined as the number of users increased as shown in Figure 4-6 and Figure 4-7. This decline can be reasoned as visualizing the same bandwidth being shared by more users, this would only reduce the

University of Hertfordshire, 2011

overall system performance. Therefore; to attain a minimum optimum performance, current MIMO-CDMA systems usually define user thresholds for a minimum system performance.

The most significant findings from the combination of multiuser MIMO with OFDM is it offers a spatial sharing of the available channel bandwidth between users. This is also done using additional hardware such as antennas. In essence, a transmitting base station can achieve spatial multiplexing gains without the cost of additional bandwidth. An immediate advantage can be seen in this setup as it opens the realization of the use of cheaper remote user terminals.

There is an increase in BER rate at corresponding SNR values for the different set of MIMO antenna utilised. The relation follows the predicted relationship derived from the MIMO attribute of improving spectral efficiency. This is reflected by the increase in BER for any particular operating frequency shown in Figure 4-8 and Figure 4-9.

The capacities offered by MIMO-OFDM compared to SISO-OFDM seem to have a linear relation in correlation with theoretical assumptions of capacity. The capacity of an OFDM system is linearly increased as the number of antennas utilised. This is because the data rates are increased while transmitting at the same bandwidth.

Another parameter varied was the total number of sub-carriers. Theoretically, increasing the sub-carrier index would not increase the system capacity; it would simply affect the symbol rate of the effective sub-carriers. A longer sub-carrier symbol rate is normally implemented as a resource to combat multipath mitigation [67] hence it is a very important specification in OFDM standards such as WiFi and WiMaX.

It can be seen clearly from Figure 4-10 and Figure 4-11 that increasing the guard band would effectively improve signal quality as delay spread is essentially improved. This increase has negligible effects on BER as seen in the difference between Rate II and Rate III although it is quite significant when compared to operation at higher SNR values as shown by Rate I systems. At higher SNRs which translates to a higher operating power, the effect of the incident inter symbol interference increases. This is seen as an increased deviation from the

other MIMO-OFDM systems (i.e. Rate II and III). Hence, a trade-off exists between the choice of guard interval length and data rate required when considering modern day systems.

5   Sphere Decoder (SD) for MIMO Detection

5.1   Introduction

The sphere decoder is a very novel technique that has been making a great impact within modern day telecommunication systems. Its main attraction is an alternative to the complexity of the maximum likelihood, ML detection algorithm. In modern times, signals are transmitted using digital modulation such as n-PSK or QAM; whose signal space-time diagram forms a constellation diagram.

In the presence of additive white Gaussian noise, the ML algorithm needs to search all the available constellation points within the channel to obtain the right one associated with the random data looking to be detected. This search can become very exhaustive and therefore makes the computational complexity of this optimal decoding algorithm increase exponentially with respect to the length of the codeword involved. This exhaustive search prompted research into means to reduce it, hence the emergence of the sphere decoding algorithm [3].

The Sphere Decoding algorithm searches the closest lattice point to the received signal within a chosen sphere radius, where each codeword would be represented by a lattice point within a lattice field [2]. A two dimensional example of this lattice search is shown in Figure 5-1 below for a 16 point signal *constellation* map. A circle is drawn around the received signal just big enough to enclose a lattice point which eliminates any other search for points outside the circle.

University of Hertfordshire, 2011
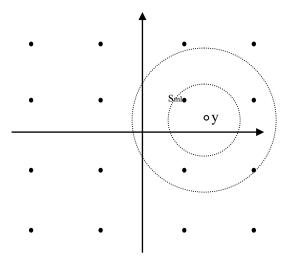
Figure 5-1:   Geometric Representation of the Sphere Decoding Algorithm

This chapter begins by explaining the concept of maximum likelihood detection and its complexity issues to show the need for a better approach to the ML algorithm. The Sphere Decoding Algorithm (SDA) presented in [1] is investigated in comparison to other MIMO detectors. A Proposed Sphere Decoding Algorithm, PSDA which is a modification of a general SDA in [1], is implemented and investigated in comparison with other sphere detectors to analyze its performance capabilities and system complexities. The scenario being assumed is a linear Space time block code (STBC) environment where the encoded data is split into N_t sub-streams which are in turn transmitted simultaneously via N_t antennas. In essence, it means that the received signal is actually a linear superposition of the simultaneously transmitted N_t sub-streams that have been corrupted by noise and channel inter-symbol interference (ISI). We also assume perfect channel knowledge at the receiver.

University of Hertfordshire, 2011

5.2   Maximum Likelihood Detection

Let us consider a linear MIMO system where a signal is transmitted using a digital modulation technique such as BPSK and QPSK. The transmission channel can be envisaged as shown in Figure 5-2.
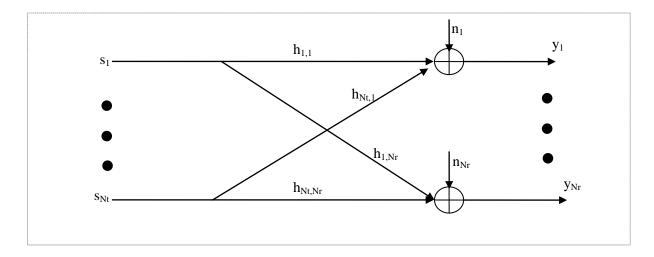
Figure 5-2:   Linear representation of a MIMO Channel

From Figure 5-2, the manner at which the MIMO channel coefficients interact with the transmitted signal is witnessed. It is assumed that the transmitter would send N_t symbols during the same time slot which leads to the incidence of N_r symbols at the receiver for any given time slot. At the receiver, the incident N_r symbols experience noise which is also indicated in the figure. Using the above Figure 5-2, we can also re-establish the relation developed in (3.1) of chapter 3 in simple matrix form as seen in (5.1) below.

$$y = Hs + n \tag{5.1}$$

University of Hertfordshire, 2011

where   *y* represents the received signal vector

               H represents the channel matrix

               s represents the transmitted symbols

               n represents the incident noise

During transmission, the actual value of the transmitted signal constellation is shifted by noise. The aim of the receiver is to estimate as close a value to the transmitted symbol as possible. In essence, the receiver would need to decide on which value of the signal constellation is closest to the actual value of the transmitted signal.

A few assumptions are implemented; the transmitted symbols, s_{Nt} are chosen from a signal constellation with an alphabet size χ and the channel matrix coefficients are known at the receiver. The transmitted symbols are normally modelled as independent and identically distributed; *iid* random variables since each random variable utilised possesses the same probability distribution as the other variables where all the variables are mutually independent of each other [2]. These symbols are uniformly distributed across the constellation alphabet, χ whose signal constellation is assumed to be centred at zero.

In essence, the ML detector tries to reduce the probability of detecting a wrong constellation point as represented in (5.2).

$$\bar{s} = \arg \max_{s \in \chi^{Nt}} P(\text{symbol vector sent} \,|\, \text{symbol vector observed}) \qquad\qquad (5.2)$$

Equation (5.2) is generally known as the *Maximum A posterior Probability*, *MAP* detection rule [19]. Also, since the probability of error in choosing the correct estimate, $\bar{s}$ is more or less equivalent to maximizing the probability of correctly estimating the received

83

signal vector, y [2]; one can utilise this attribute; i.e. $P_e(s = \bar{s} \mid y, H)$, as shown in (5.3) where it has been expanded to analyse it further.

$$P_e(s = \bar{s} \mid y, H) = \frac{P(s = \bar{s}) f_{y|s,H}(y \mid s = \bar{s}, H)}{f_{y|H}(y \mid H)} \tag{5.3}$$

where $f_{y|H}$ is the conditional probability density function of y given values for H

$f_{y|s,H}$ is the conditional probability density function of y given values for s and H

Consequently, as the values of $P(s = \bar{s})$ and $f_{y|H}(y \mid H)$ do not rely upon the value of $\bar{s}$, it implies that $P_e(s = \bar{s} \mid y, H)$ can be maximised for $\bar{s}$ [2]. This would in turn maximise the $f_{y|s,H}(y \mid s = \bar{s}, H)$ term in (5.3) which transforms into the well-known ML detector criterion in (5.4) where $\bar{s}_{ML}$ represents the ML estimate.

$$\bar{s}_{ML} = \arg \max_{s \in \chi^{Nt}} f_{y|s,H}(y \mid s = \bar{s}, H) \tag{5.4}$$

The received vector model adopted in (5.1) can be used in conjunction with (5.4) to establish the relationship [2] depicted in (5.5).

$$f_{y|s,H}(y \mid s = \bar{s}, H) = f_n(y - H\bar{s}) \tag{5.5}$$

University of Hertfordshire, 2011

where f_n represents the probability density function of white Gaussian noise.

A standard Gaussian noise vector, n can be visualised as a collection of N_r independent and identically distributed (i.i.d) Gaussian random variables (n_1 , n_2 , ... , n_{Nr}). It is well known that the probability density function of white Gaussian noise is given by (5.6).

$$f_n(\bar{n}) = \frac{1}{(\pi\sigma^2)^{N_r}} e^{-\frac{1}{\sigma^2}\|\bar{n}\|^2} \tag{5.6}$$

Recalling that a means of maximising $f_{y/s,H}$ is by minimising the calculated Euclidean distance, $\|\bar{n}\|^2$; it follows that we can substitute $\bar{n}$ with $\bar{n} = y - H\bar{s}$ which leads to very well known equation representing the ML estimate of s [1], [2] given by (5.7).

$$\bar{s}_{ML} = \arg\min_{s \in \chi^{Nt}} \| y - H\bar{s} \|^2 \tag{5.7}$$

It can be seen clearly that the ML detector attempts to retrieve the desired constellation point, $\bar{s}_{ML}$ that would minimise $\| y - H\bar{s} \|^2$. In essence, an ML detector needs to calculate $\| y - H\bar{s} \|$ for every transmitted constellation point before deciding on which symbol was sent. Although the ML estimate is a very accurate means of estimating the transmitted symbols, it is clear that for higher order systems where N_t or constellation size, m is high, the computational complexity of ML would become very significant.

This ML estimate, $\bar{s}_{ML}$ embodies the daunting nature of the computational complexity witnessed in modern day telecommunication systems to achieve a ML detection of the transmitted signal in scenarios of large m and N_t. This is usually termed as being NP-Hard

85

[30]. The high computational complexity necessary for ML detector operation led to research into other detection algorithms which offer much lower complexity though they might be sub-optimal in nature. A derivative of ML detection was presented by Fincke-Pohst (F-P) and Schnorr-Euchner (S-E) who devised computationally efficient techniques to derive a sub-optimal ML estimate without the need of the exhaustive search across all constellation points exhibited by normal ML detection algorithm [32], [36]. This algorithm searches for the required ML estimate within a hyper-sphere in the signal constellation mapping as was seen in Figure 5-1 leading to the *sphere decoder* becoming the industry name for detectors based on algorithms using this manner of sphere search. A number of sphere detectors currently exist but most usually utilise either a F-P or S-E algorithm as the foundation of their operation [36].

5.3 Principle of the General Sphere Decoder Algorithm

The sphere decoder is derived from a variation of the ML equation shown in (5.7). Another way to look at (5.7) is to refer to the Euclidean distance, d_E which can be expressed as shown below.

$$d_E = | y - H\overline{s} | \tag{5.8}$$

where d_E represents the Euclidean distance.

During transmission through a communications channel, the received symbol is simply one of the constellation points displaced by noise. A ML decoder calculates the Euclidean distance; i.e. the distance between the received symbol and any point on the constellation map. Therefore, ML attempts to find the Euclidean distances between the received symbol and all points on the constellation map before selecting the minimum out of the calculated distances as it would obviously be the closest match on the constellation map to the received symbol.

A sphere decoder limits the number of constellation points utilised in order to calculate $\bar{s}_{ML}$ by limiting the symbol search to occur within a hyper-sphere with a radius, d_r around the received signal vector, y. The radius of the hyper-sphere is chosen in such a manner to maintain the presence of at least one constellation point within it. It is obvious that if the closest point lies within the hyper-sphere, it would generally represent the closest point of the whole constellation lattice and in effect would have avoided the extra computational complexity caused by the need for an ML detector to search the whole lattice [34] as depicted in Figure 5-1 above.

From the principle of SD above, it is obvious that a very important design attribute would be the actual radius of the sphere. This is a very tricky design question and different sphere decoders adopt different means of generating the search radius, d_r. The choice of d_r would affect the complexity of the system because if d_r is too large, it would have an adverse effect on the system as there would be too many constellation points to search through and in effect the aim of SDAs in trying to reduce ML complexity is nullified. Also at the other extreme, if d_r is too small, there is a possibility of not finding any constellation point within that sphere and hence a flawed system. Geometrically speaking, the obvious solution would be to calculate the smallest radius of spheres centred at the lattice points that would basically cover the entire space. This is known as the *covering radius* [41]. Calculating this radius involves a lot of increased complexity and also effectively removes the aim of SDAs if deployed as the choice of radius selection [41].

University of Hertfordshire, 2011

5.3.1 System Model of a Sphere Decoder

To consider the SDA algorithm, QR decomposition is performed on the channel coefficients. It is known that $H = QR$ where Q is a unitary orthogonal matrix and R is an upper triangular matrix whose diagonal possesses real valued positive entries [36].

Recall (5.1):

$$y = Hs + n$$

Since Q is unitary implying $Q^H Q = I$, multiplying both sides by Q^H turns (5.1) into (5.9) below:

$$x = Rs + Q^H n \tag{5.9}$$

where $x = Q^H y$

Using (5.9), (5.7) can be represented as shown in (5.10) below.

$$\bar{s}_{ML} = \arg \min_{s \in \chi^{Nt}} \| x - R\bar{s} \|^2 \tag{5.10}$$

The manner at which an SDA works is basically solving (5.10) where it can be clearly seen that in order to achieve correct results, the utilised SDA algorithm needs to completely identify all the constellation points that exist within the hyper-sphere with a radius, d_r centred around a received vector point, x. Using (5.10), a relationship can be established between d_r and x as seen in (5.11). Therefore, a lattice point $H\bar{s}$ would exist in a sphere of radius, d_r if and only if the condition of (5.11) is met.

$$d_r^2 \geq \| x - H\bar{s} \|^2 \tag{5.11}$$

It is possible to derive an alternative solution using the QR factorization of H and substituting for H as shown in (5.12) similar to the initial algorithms utilised by Fincke and Pohst [32].

$$d_r^2 \geq \| x - [Q_1 \; Q_2] \begin{bmatrix} R_1 \\ R_2 \end{bmatrix} \bar{s} \|^2 \tag{5.12}$$

where Q_1 and Q_2 represent the first N_r and last $(N_r - N_t)$ columns of the Q unitary matrix and $R_2 = 0$. Using this unitary quality of the Q matrix, we can redefine (5.12) as (5.13).

$$\| x - [Q_1 \; Q_2] \begin{bmatrix} R_1 \\ 0 \end{bmatrix} \bar{s} \|^2 = \| \begin{bmatrix} Q_1^H \\ Q_2^H \end{bmatrix} x - R_1 \bar{s} \|^2$$

$$= \; \| Q_1^H x - R_1 \bar{s} \|^2 + \| Q_2^H x \|^2 \tag{5.13}$$

Equation (5.12) can then be rewritten using (5.13) to establish the relationship in (5.14).

$$d_r^2 - \| Q_2^H x \|^2 \geq \| Q_1^H x - R_1 \bar{s} \|^2 \tag{5.14}$$

For clarity purposes, we assume $z = Q_1^H x$ and $\Delta d^2 = d_r^2 - \| Q_2^H x \|^2$; we can then re-write (5.14) as (5.15).

$$\Delta d^2 \geq \| z - R_1 \bar{s} \|^2 \tag{5.15}$$

$$\Delta d^2 \geq \sum_{i=1}^{N_t} (z_i - \sum_{j=i}^{N_t} r_{i,j} s_j)^2 \tag{5.16}$$

where $r_{i,j}$ represents the $(i,j)^{th}$ entry of R_1

s_j is the jth bit of symbol, s

Following an expansion of (5.16), we obtain (5.17) below.

$$\Delta d^2 \geq (z_{N_t} - r_{N_t,N_t} s_{N_t})^2 + (z_{N_t-1} - r_{N_t-1,N_t} s_{N_t} - r_{N_t-1,N_t-1} s_{N_t-1})^2 + \ldots \tag{5.17}$$

University of Hertfordshire, 2011

It is noticed that in (5.17), the first term is the only term whose value is dependent on a single bit of *s* while the second term depends on two bits of the symbol *s* and so on. Therefore, it is possible to assume that s_{Nt} would belong to the interval depicted in (5.18).

$$\left\lceil \frac{-\Delta d + z_{N_t}}{r_{N_t,N_t}} \right\rceil \leq s_{N_t} \leq \left\lfloor \frac{\Delta d + z_{N_t}}{r_{N_t,N_t}} \right\rfloor \tag{5.18}$$

It should be noted that $\lceil : \rceil$ represents rounding out to the larger of the elements in the set of numbers that cover the selected lattice points [14], [15], [32] and $\lfloor : \rfloor$ represents rounding off to the smaller of the elements in the set of numbers that cover the selected lattice points [14], [15].

The second term depends on two terms which leads to the possibility of re-defining a new set of boundaries for s_{Nt-1} taking into account the effect of an already calculated s_{Nt} using the new definitions below to establish a new interval (5.19) for s_{Nt-1}. This is done with the consideration that (5.18) would have already been observed.

$$\Delta d_{N_t-1}^2 = \Delta d^2 - (z_{N_t} - r_{N_t,N_t} s_{N_t})^2$$

$$z_{N_t-1|N_t} = z_{N_t-1} - r_{N_t-1,N_t} s_{N_t}$$

$$\left\lceil \frac{-\Delta d_{N_t-1} + z_{N_t-1|N_t}}{r_{N_t-1,N_t-1}} \right\rceil \leq s_{N_t-1} \leq \left\lfloor \frac{\Delta d_{N_t-1} + z_{N_t-1|N_t}}{r_{N_t-1,N_t-1}} \right\rfloor \tag{5.19}$$

University of Hertfordshire, 2011

This same interval limit can be adjusted in a similar manner to find all the remaining bit components of s from s_{Nt} to s_1 [32]. These interval limits are used to correctly enumerate all the lattice points required for (5.11).

5.3.2   General Sphere Decoder Algorithm

A suitable code can be written as indicated below to implement a general sphere decoding algorithm as discussed above.

- Required inputs: $Q = [Q_1 \quad Q_2], R, x, z = Q_1^H x, d_r$

- (1): Set initial layer $k = N_t, \Delta d_{N_t}^2 = d_r - \| Q_2^H x \|, z_{N_t|N_t+1} = z_{N_t}$

- (2): Set upper bounds (UB) for s_k

$$UB(s_k) = \left\lceil \frac{\Delta d_k + z_{k|k+1}}{r_{k,k}} \right\rceil ;$$

$$s_k = \left\lfloor \frac{-\Delta d_k + z_{k|k+1}}{r_{k,k}} \right\rfloor - 1;$$

- (3): Increase s_k unit wise $s_k = s_k + 1$

If $s_k \le UB(s_k)$ jump to (5) else continue to (4)

- (4): Increase k unit wise $\qquad\qquad k = k + 1$

    If $k = N_t + 1$; end algorithm, else go back to (3).

- (5): Decrease k unit wise; If k = 1, jump to (6) else define new values below

    $k = k - 1$

    $$y_{k|k+1} = y_k - \sum_{j=k+1}^{N_t} r_{k,j} s_j$$

    $$\Delta d_k^2 = \Delta d_{k+1}^2 - (y_{k+1|k+2} - r_{k+1,k+1} s_{k+1})^2$$

    Go back to (2)

- (6): A solution has been discovered.

    Save s and its distance from x; $\Delta d_{N_t}^2 - \Delta d_1^2 + (y_1 - r_{1,1} s_1)^2$

    Go back to (3).

University of Hertfordshire, 2011

The algorithm described above can be envisaged in the manner of a tree search algorithm [31]. This is a widely recognised manner of interpreting the search characteristic employed by a typical sphere decoder. In other words, the *shortest path* along a *tree* corresponds to finding the minimum Euclidean distance and hence it results in finding the ML solution for the received vector. A tree structure for a 2-by-2 MIMO system is shown below in Figure 5-3.
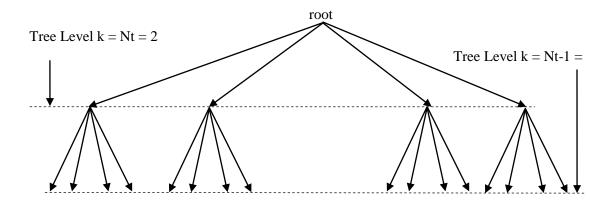
Figure 5-3:   Tree search representation for a 2-by-2 MIMO SD-QPSK system

The ML detector involves an exhaustive search from the root via all the branches to all the nodes in the tree representation in Figure 5-3 above. The aim of SDA is to limit the branches visited to establish the maximum likelihood solution required. A constellation point is depicted by a node on the tree diagram; therefore, the path from the root to end node (leaf node in some literature) [15], [31] can be visualised as a possible solution. Therefore, the path with the smallest path equates to the solution which would possess the minimum Euclidean distance required.

Examining Figure 5-3, it can be visualised how the complexity of SD is reduced using tree pruning techniques. This is simply because since every node visited is associated with its own Euclidean distance; referred to as partial Euclidean distances, PED's in other literature.

If the visited node's Euclidean distance is larger than the search radius of the sphere, it simply implies the branches connecting the node to the root are also outside the search radius and can thus be neglected or pruned from the tree. This continues at the leaf nodes to establish the nodes with PED's less than the search radius and effectively updating the sphere radius to this lower value [14].

There are two main adopted methods of accessing the SD tree [2],[30],[32] namely *depth-first* and *k-best* (breadth-first). The former is the basis of the Schnorr-Euchner, S-E SD algorithm and has been utilised within this project due to the lower complexity if offers over the faster approach of k-best tree search which uses parallel processing [30] to improve the search speed. The S-E SD algorithm is based on the more traditional tree search which analyses one node per cycle.

In other words, the S-E SD algorithm uses radius reduction techniques to function properly. The initial radius is normally set to begin at infinity which is indicative of an exhaustive ML search [14], [17]. The algorithm then tends to update the radius when a viable solution is found (i.e. at the leaf node). It then continues the tree search with the new radius discovered being the value of the PED just observed. Therefore, since the complexity of SD is dependent on the search radius as discussed earlier, the radius reduction offered by the S-E SDA is a very attractive feature for the deployment of SD using this algorithm [30].

5.3.3   Choice of Sphere Radius

This is one of the underlying design tradeoffs required for the successful meaningful operation of a sphere decoder. As already discussed, the complexity of a sphere decoder would vary accordingly with the size of the sphere radius. This is because the larger d_r became, the larger the range of constellation points that would need to be visited to obtain the correct set of points within the hyper-sphere, this relationship is of an exponential nature for higher values of d_r [31]. On the downside as well, if d_r is too low in value, a possibility exists whereby there would be no constellation points to search through and hence the system

95

having to return zero or search the entire constellation lattice just like a normal ML detector and this in turn defeats the purpose of using SD [30], [31].

The Schnorr-Euchler, S-E SD algorithm was utilised in preference to its Pohst counterpart mainly due to the lower complexity involved with the S-E SD algorithm as it is not dependent on the initial radius of the sphere. This is because this value is initially set to infinity [31]. Other SD algorithms use other values for d_r such as the zero forcing estimate (referred to as the Babai estimate) [14] and a scaled variance of the noise element within the system [30].

It follows that as we have obtained the channel matrix, H via channel knowledge at the receiver and due to the geometric properties of the constellation matrix, it is possible to assume the multiplication of the channel with the signal does not affect the branch lengths within the actual transmitted symbol [17]. After QR decomposition, recalling the solution $(Rs) = \bar{y}$ corresponds to the zero forcing estimate of the system which is the least squares solution to (5.7). To complete the result, we solve for $\bar{s}$ by rounding up to the closest integer value to obtain the required lattice point. This lattice point is normally identified to as the Babai estimate mentioned earlier [14] and the search radius, d_r can be defined as the difference between the received point and the Babai estimate as shown in (5.20)

$$d_r = \| R\bar{s} - \bar{y} \| \tag{5.20}$$

In modern day telecommunication systems, the channel parameters are not always known and in such a situation, the complexity of the system would increase significantly as a new unknown has been invited into the system and there would be a need to calculate the covering radius which is normally referred to as also being NP-Hard [16]. A better estimate of the initial radius can be obtained from the noise variance accompanying the system [42]. This choice meets the required criteria because the actual shift in the received symbol from

the transmitted symbol is dependent on the noise statistics of the system. The noise attribute is an independent function depicted by (5.21) below.

$$\frac{1}{2\sigma^2} \| n \|^2 = \frac{1}{2\sigma^2} \| y - Hs \|^2 \qquad (5.21)$$

where σ^2 represents the variance with a mean, μ equals zero for an AWGN scenario.

The value of d_r is chosen in such a manner to ensure that the new radius derived from (5.21) above is such that the probability of a transmitted symbol is found inside the search sphere is extremely high [36], [42]. This leads to a universal relationship also utilised in recent sphere decoder systems as seen in (5.22) given the relationship depicted in (5.21).

$$d_r^2 = \alpha N_r \sigma^2 \qquad (5.22)$$

where α is a scaling factor implemented into the system.

5.3.4   The Schnorr-Euchler SD Tree Search

The SD algorithm is a less complex algorithm used to achieve ML detection in modern telecommunication systems. This is done by interpreting the ML detection in the form of a tree search. To achieve SD, QR decomposition is done on the channel coefficients to produce the required squared matrices. It is worthwhile to note that since SD depends on

University of Hertfordshire, 2011

QR decomposition and Q needs to be a square matrix, the SD algorithm tends to fail in systems where $N_r > N_t$ [34].

The aim of the S-E SDA is to quickly recover the ML estimates while reducing the search radius during its operation to limit the node search and effectively the system complexity [36]. The S-E SDA performs a depth first search of the tree by correctly enumerating the required symbol search set. It finds the symbol estimate s_{Nt-k+1} where the search starts at the root with $k = N_t$. A strategy which was first proposed by C.P. Schnorr and M. Euchner [36] used an increasing distance from the unconstrained least squares estimate, $\bar{y}$ where

$$\bar{y} = (r_{N_t-k+1})^{-1} z_{N_t-k+1} \qquad (5.23)$$

This kind of enumeration procedure has its advantages over other methods or variants due to its radius reduction principle in sequence with its operation. The first leaf node visited is actually the zero forcing estimate i.e. the Babai estimate; this already corresponds to a very small radius at the start and hence automatically reduces the search radius as the Babai estimate should be fairly close to the required ML point. This would obviously drastically reduce the complexity of the search and makes the S-E SDA already look favourable as the daunting task of selecting a search radius is almost or completely eliminated from the design parameters [34]. The manner by which the S-E SDA operates is the reason why the initial search radius can be set to a significantly large value or infinity as a large radius would also ensure that the required ML estimate is located within the sphere and since the first node visited is at the Babai estimate, the subsequent tree search radius would also be small. After the expansion of (5.17), the increments required for use in the SD algorithm can be visualized.

$$\| z - Rs \|^2 = | z_{N_t} - R_{N_t,N_t} s_{N_t} |^2 + | z_{N_t-1} - R_{N_t,N_t-1} s_{N_t-1} - R_{N_t,N_t} s_{N_t} |^2 + ...$$

$$+ | z_1 - R_{1,1} s_1 - R_{1,2} s_2 |^2 - ... - R_{1,N_t} s_{N_t} |^2 = \sum_{i=1}^{N_t} | \Delta e_i |^2$$

The first term corresponds to a value for $| \Delta e_i |^2$ where $i = N_t$, the second term for when $i = N_{t-1}$ and the last term depicted is for $i = 1$. These can be visualised as distance increments from successive layers whose sums are calculated recursively from the root level where $k = N_t$ to the leaf node where $k = 1$ as shown in (5.24).

$$| \Delta e_i |^2 = | z_i - \sum_{k=i}^{Nt} R_{i,k} s_k |^2 \tag{5.24}$$

As the name suggests, these *partial sums*, generically referred to as partial Euclidean distances, PEDs [30] represent the distance from the received vector point to the node of interest. The PEDs can thus be calculated and updated using (5.25) and (5.26) below.

$$\Delta d_i = \sum_{k=i}^{N_t} | \Delta e_k |^2 \tag{5.25}$$

$$\Delta d_i = \Delta d_{i+1} + | \Delta e_i |^2 \tag{5.26}$$

University of Hertfordshire, 2011

An initial condition is set as such where $\Delta d_{N_t+1} = 0$. After obtaining the PEDs, it is easy to prune the tree during the search because if we ever arrive at a node which possesses a PED larger than the current sphere radius, d_r, it simply indicates the sub-tree of that node does not need to be searched as going through that sub-tree only increases the search distance which has already been found to be outside the sphere radius and not the required ML point of interest [36].

There are different variants of the tree search method currently recognised where the manner and direction of the search are different to the S-E SDA [36], an example is the *Stack Sphere Decoding Algorithm* developed by F. Jelinek [38] although for all SD algorithms, the tree search normally begins at the root level.

5.4   Simulations

Simulations were carried out using MATLAB version R2009a to establish a sphere decoder using modulation techniques such as QPSK, 16-PSK, 32-PSK and 64-PSK for transmission. These were adapted to different MIMO antenna configurations and their performance analysed. A general sphere detector was compared to the MIMO detectors discussed in previous chapters to determine the high performance and complexity involved in general sphere decoder algorithms, GSDAs.

5.4.1   Comparison with other Detectors

A sphere detector based on the Schnorr Euchner algorithm was investigated using the MIMO configuration and the performance in terms of BER was compared with versions of VBLAST; i.e. ZF-OSIC and MMSE-OSIC, and the ML receiver. A user signal was

implemented with the MIMO algorithm for different antenna configurations. The modulation methods tested was mainly QPSK and some variants of n-PSK with a total number of modulated bits, $n_{bits} = 1 \times 10^5$. Figure 5-4 shows the results achieved where it is seen that a sphere decoder can achieve ML detection.
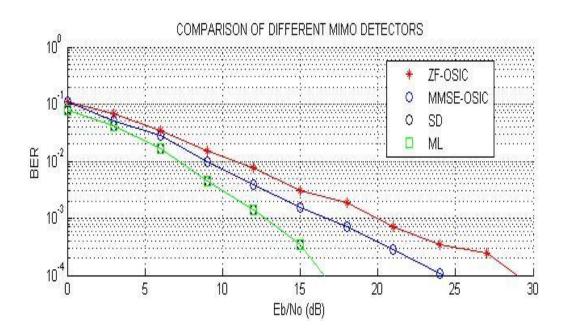
Figure 5-4:   BER using QPSK modulation at the transmitter

Figure 5-4 shows the BER performance for a 2-by-2 MIMO system where different versions of VBLAST; ZF-VBLAST & MMSE-VBLAST have been compared against both a sphere decoder based on the Schnorr & Euchner algorithm and a maximum likelihood detector. A QPSK modulated signal was used simply due to its recognised implementation as a modulation technique adopted in technologies such as IEEE 802.11 WiFi, IEEE 802.16 WiMAX, WCDMA/HSDPA 3G and 4G [1], [36], [37].

101
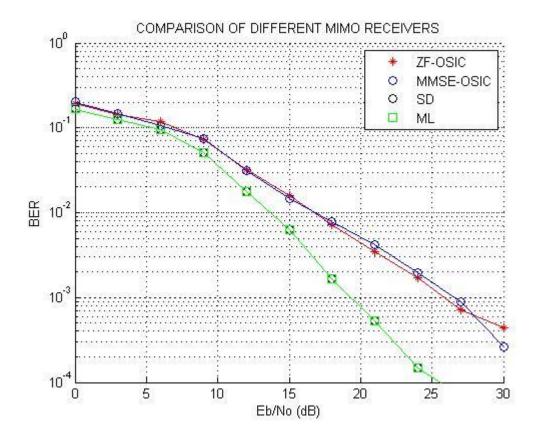
Figure 5-5:   BER using 16-PSK at the transmitter

The current industrial telecommunication standards normally support QPSK up until 64-PSK and 64-QAM. Figure 5-5 shows the BER performance achieved with a slight modification in the MIMO system of Figure 5-4 where the 2-by-2 MIMO system used 16-PSK for a system transmitting a total number of bits equalling 1×10^4.

5.4.2   Visited Nodes for different Antenna Configuration

The sphere decoder algorithm based on principles developed by Schnorr & Euchner [1] achieved ML detection as seen in 5.4.1. There was an obvious hindrance derived from the runtime of the simulations as expected. As there is a need to perform an exhaustive search when using the ML detector; in essence, the whole aim of the sphere decoding algorithm

would be to reduce the time taken in calculating the maximum likelihood estimate for a received symbol. This increased simulation time is caused by the need to search through all the constellation points which is typical of a ML detector. The complexity can generally be visualised as being related to the search radius of the ML detector. Therefore, decreasing the search radius as witnessed in the SD algorithm should in effect lower the runtime and hence lower the complexity of the system. Different configurations of the general sphere decoder algorithm were examined and their results compared to the modified SDA. The total number of visited nodes corresponds to the total number of constellation points searched; therefore reducing the radius would also reduce this value as witnessed in Figure 5-6 below where a ML detector was compared to a General Sphere decoder (GSD) based on the S-E iterations with the initial radius set to infinity.
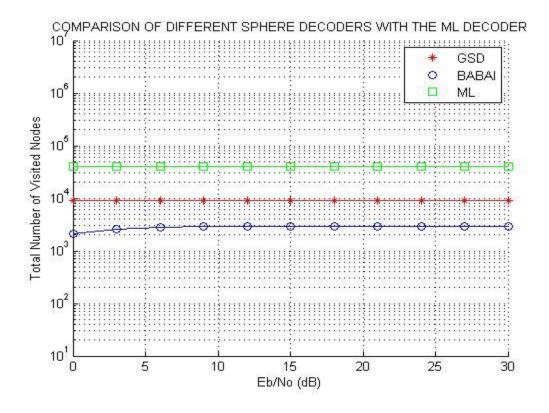
Figure 5-6: Comparing the Total Number of Nodes for Different Sphere Detectors

University of Hertfordshire, 2011

5.4.3 S-E SDA using a modified Babai radius

The GSD sets the initial radius search to begin from infinity to allow the sphere to always encompass the required zero forcing estimate at the first node. Using the means described in (5.19), it should be noted that rounding off to nearest integer value occurs and therefore, computation errors need to be taken into account when the value of N_T or m increases. At some values of N_T, the sphere detector based on the Babai radius failed to return a value as there were no points inside the sphere and hence returned with no value on higher values of N_T. To overcome this, there was a need to slightly increase the search radius using a unit increase by introducing a scaling factor, *rt*. The modified sphere decoder was found to achieve a 100% success rate with respect to always locating a constellation point within the search sphere for a transmission with $n_{bits} = 1 \; x \; 10^4$.
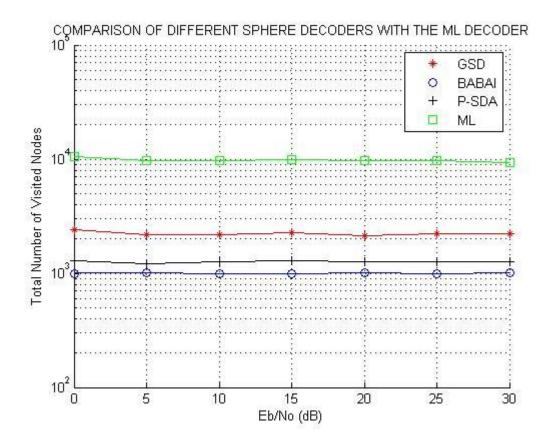
Figure 5-7:   Comparing the Total Number of Nodes with $m = 2$, $rt = 1$, $N_t = N_r = 2$.

Figure 5-7 above also includes the total number of nodes that have been visited assuming the search radius was the Babai estimate. It is used as a point of reference to compare how much complexity is added to the system by utilising the modified radius in the Proposed SDA (PSDA). This reference has been applied to Figures 5-8, 5-9 and 5-10 where different values of m, N_t, N_r and rt have been deployed for different system configurations to determine the robustness of the proposed SDA.

University of Hertfordshire, 2011
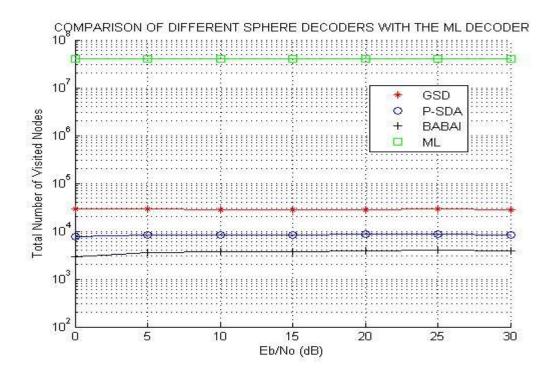
Figure 5-8: Comparing the Total Number of Nodes with $m = 4$, $rt = 2$, $N_t = N_r = 4$.
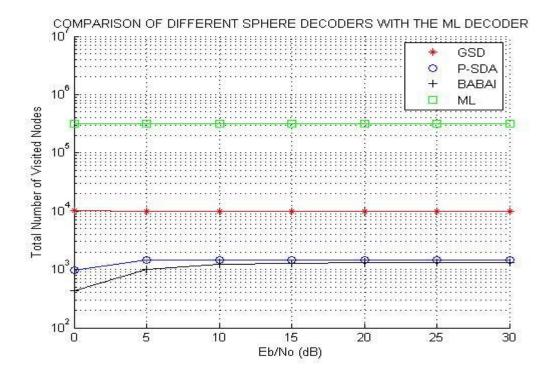
Figure 5-9: Comparing the Total Number of Nodes with $m = 2$, $rt = 1$, $N_t = N_r = 4$.
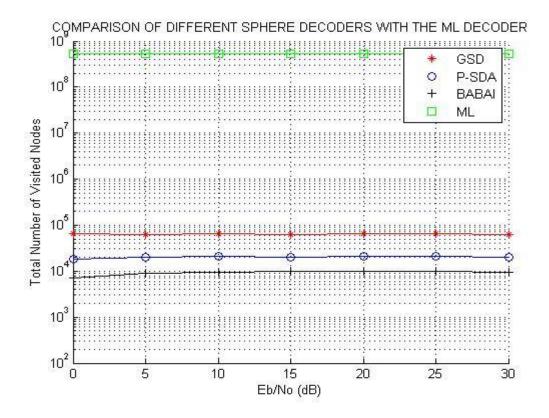
Figure 5-10: Comparing the Total Number of Nodes with $m = 5$, $rt = 2$, $N_t = N_r = 4$.

It is clear from Figure 5-7, 5-8, 5-9 and 5-10 that the P-SDA adds a slight complexity increase with respect to comparison with an SE-SDA based on the Babai radius. This increase is visualised by the increased amount of nodes visited for the different scenarios evaluated. Tables 5-1, 5-2 and 5-3 have been drafted below to include the total number of visited nodes and the different failure and success rate patterns exhibited for different antenna configurations corresponding to $N_t = N_r = 2$ and 4 respectively.

University of Hertfordshire, 2011

BER	rt = infinity	rt = 1	rt = 2	rt=1 (PASS/FAIL)	rt=2 (PASS/FAIL)
10 dB	9115	4096	5120	PASS	PASS
15 dB	9179	4127	5225	PASS	PASS
20 dB	9137	4128	5202	PASS	PASS
25 dB	9158	4097	5148	PASS	PASS
30 dB	9062	4143	5149	PASS	PASS

Table 5-1:   Total number of nodes with $N_t = N_r = 2$, m = 2 and $N_{tot} = 10^4$

BER	rt = infinity	rt = 1	rt = 2	rt=1 (PASS/FAIL)	rt=2 (PASS/FAIL)
10 dB	16705	9486	11200	PASS	PASS
15 dB	16734	9284	11045	PASS	PASS
20 dB	17032	9611	11413	PASS	PASS
25 dB	16933	9456	11200	PASS	PASS
30 dB	16579	9406	11104	PASS	PASS

Table 5-2:   Total number of nodes with $N_t = N_r = 2$, m= 4 and $N_{tot} = 10^4$

BER	rt = infinity	rt = 1	rt = 2	rt=1 (PASS/FAIL)	rt=2 (PASS/FAIL)
10 dB	27973	Error	8451	FAIL	PASS
15 dB	28255	Error	8302	FAIL	PASS
20 dB	28564	Error	8606	FAIL	PASS

University of Hertfordshire, 2011

25 dB	28963	*Error*	8612	FAIL	PASS
30 dB	28497	*Error*	8462	FAIL	PASS

Table 5-3:　　　Total number of nodes with $N_t = N_r = 4$, m= 4 and $N_{tot} = 10^4$

Tables 5-1, 5-2 and 5-3 were populated using the corresponding values where *Error* was displayed when the search sphere contained no points within it. The test was to ensure that for a certain value of *rt*, the system would actively have at least one point within the search sphere. A *PASS* was displayed when this condition was met and a *FAIL* otherwise.

5.5　　Summary and Analysis

The time taken by the conventional ML receiver to process was significantly longer than any other method and sometimes took hours to finish depending on the total number of bits that were transmitted. The GSD was significantly more responsive with regards to the conventional ML detector. Figures 5-4 & 5-5 show that the GSD achieves ML detection. The reason of so much interest in SDAs is simply because they reduce the complexity of finding the ML estimate of a received signal which is generally termed to be NP-Hard. The search sphere has been identified to be a very important decision factor in the design of SDAs as it basically decides the complexity of the overall system as it is reduces the nodes visited. This can be witnessed in Section 5.4.2 above where each visited node corresponds to a trip from a root to a node. This is also regarded as a means of measuring the complexity of a ML detector. Therefore reducing the amount of nodes visited effectively reduced the run time and in essence, the computational complexity required for ML detection.

The sphere radius is an important quantity and despite its importance, it has no exact definition for its value and is usually estimated. The GSDA uses methods based on a Schnorr-

Euchner lattice reduction algorithm as already described. This method sets the initial radius to infinity although this is only for the first trip to a visiting node as this would guarantee a point definitely within the search sphere at initialisation. This first visited node is generally termed the Babai estimate.

The telecommunication industry today adopts a different approach to defining the initial radius, d_r as the Babai estimate where pre-processing before the search commences to define a value for the search radius as discussed in Section 5.3.4. The search for the Babai estimate is normally done to the nearest symbol and therefore leads to computational errors as witnessed in our experiments by the *FAIL* result which indicates that not 100% of the received symbols were decoded. This is caused by the rounding off errors incurred when calculating the Babai estimate. The proposed SDA, P-SDA utilises a variable; *rt*, to slightly increase the search radius to allow for the increased efficiency of a 100% successful detection without the need to use an initial big radius as the GSD and in effect slightly increase the complexity. Different values of *m, N_t, N_r* and *rt* were implemented to try to notice and establish a suitable relationship to define rt. It was noticed from Table 5-1, 5-2 and 5-3 that the system demanded a minimum of a unit increase to get a *PASS*. This result was unaffected by varying the values of *m* and obviously increasing *rt* should make no difference as it only increases the search radius. A trend and relationship was noticed between N_t and *rt* where in order to get a 100% success rate of detection where a PASS is awarded, the value for rt for minimum complexity is: $rt = N_r / 2$. This value for *rt* is independent of the utilised value of *m*.

6   Conclusions and Future Work

6.1   Conclusions

This thesis investigated the examples of the different types of receivers utilised within a wireless communication system. It analysed linear and non-linear receivers to evaluate their performance attributes and the effect of varying certain transmission parameters such as modulation order and digital modulation type.

The contribution of MIMO to the wireless communication industry was also examined by initially investigating the performance of various MIMO receivers utilised within the wireless industry. A V-BLAST MIMO Receiver was combined with two well know modulation techniques in CDMA and OFDM to investigate the improvements envisaged while adopting MIMO technology.

A Sphere decoder based on the Schnorr-Euchner algorithm was implemented to obtain a maximum likelihood solution of the transmitted symbol at the receiver. This decoder along with other MIMO Receivers was compared to a conventional ML receiver by comparing their BER performance. The Sphere decoder was modified to overcome an impairment normally overlooked in the general equation for calculating the radius of the search sphere. The modified sphere decoder was compared to other sphere decoders and the ML decoder by counting the total number of nodes visited during detection. This established an insight into the complexity issues slightly reduced by adopting a Sphere decoder for ML detection.

6.1.1 Effect of MIMO on BER performance

It is safe to conclude that MIMO increases the BER performance of the receiver. The addition of MIMO to conventional 3G, LTE and 4G systems using CDMA or OFDM has been researched extensively. OFDM and CDMA are modulation techniques that currently have an edge over simpler digital modulation techniques such as BPSK, QPSK, QAM and n-PSK. It has been easily established from the results the effect of the addition of MIMO to the system. MIMO increases the spectral efficiency of the system and generally the achieved BER performance linearly increases proportionally to the number of receive antennas deployed. MIMO-OFDM and MIMO-CDMA deliver better data rates to their SISO counterparts.

6.1.2 Improved BER performance

An aim of this project was to identify and implement a receiver showing improved bit error rates by comparing the performance of several industrially recognised receivers. Two variations of receivers were tested which led to an observation of achieving improved BER performance when both variants of a non-optimal receiver were utilised in sync with each other such as the MMSE linear detector and its addition with the non-linear OSIC for use in a V-BLAST receiver. This detector combination offered the best BER performance achieved when trying to achieve a non-optimal solution for the received signal. The conventional optimal receiver achieves ML detection with very high computational complexity and therefore poses a difficult conundrum with respect to operating at higher digital modulation rates as higher rates correspond to a longer search cycle and hence very large and unwanted runtimes. Hence, though the optimal ML receiver achieves the best BER performance, it is not an attractive solution for systems involving orders of higher modulation.

University of Hertfordshire, 2011

6.1.3   Complexity of a ML decoder

A modification of the general sphere decoder (GSD) has been presented in this thesis as exhibiting the best BER performance out of the non-linear and linear receivers tested. It was shown that the sphere decoder achieved a ML solution at a reduced complexity to the conventional ML detector. The GSD is based on the Schnorr Euchner algorithm which sets the initial search radius to infinity to allow for the *100%* probability of obtaining a point within the sphere. A modification to the GSD is utilised in the industry where the Babai estimate was utilised to find the search radius. The proposed modification of the Babai estimate realised a *100%* probability of finding a point within the search sphere was maintained.

6.2   Future Work

The future of telecommunications is nearing towards the realization of the 4G standard as defined by the International Telecommunications Union (ITU) where peak data rates of 100 Mbps and 1Gbps have been targeted for high and low mobile service operation respectively. MIMO-CDMA and MIMO-OFDM have been shown to realise significant BER performance improvement compared to their SISO counterparts.

6.2.1   MIMO and MC-CDMA

The combination of OFDM and CDMA; known as multicarrier CDMA, MC-CDMA is currently a very attractive technology in the wireless industry due to the advantages it offers over constitute technologies i.e. OFDM and CDMA. A combination of MIMO with

MC-CDMA should make significant BER improvements when compared to MIMO-OFDM or MIMO-CDMA.

6.2.2   Modified Sphere Decoder (M-SDA)

The received signal has a relation to its associated noise variable. This noise variable has the same statistics as the received signal and can be used to determine a value for the search radius. The initial radius is set to a scaled variance of the associated noise variable. This can be researched and investigated to establish an M-SDA. The total number of nodes visited should then be compared to the P-SDA to establish any system complexity improvement.

6.2.3   Sphere Decoder and MC-CDMA

A choice of a receiver based on the M-SDA or P-SDA should be made against two decision statistics namely observing a *PASS* and a probability of *100%* as described in Chapter 5. This choice should be used as the detector to evaluate the combination of MC-CDMA with MIMO.

7   References

[1]   B. Hassibi and H. Vikalo, "On the Sphere Decoding Algorithm I: Expected Complexity", IEEE Transactions on Signal Processing, vol. 53, no. 8, pp. 2806-2818, Aug. 2005

[2]   H. Vikalo, Sphere Decoding Algorithms for Digital Communications. PhD Thesis, Stanford University, 2003.

[3]   P. W. Wolniansky, G. J. Foschini, G. D. Golden, R. A. Valenzuela, "V-BLAST: An Architecture for Realizing Very High Data Rates Over the Rich Scattering Wireless Channel", Signals, Systems, and Electronics, URSI International Symposium, 1998. Pages: 295 - 300

[4]   S. Verdu, "Minimum Probability of Error for Asynchronous Gaussian Multiple Access Channels," IEEE Trans. Info. Theory, vol. IT-32, no.1, pp 85 -96, 1986.

[5]   F. B. Gross, Smart Antennas for Wireless Communications with Matlab, McGraw-Hill, 2005

[6]   B. M. Hochwald and S. Brink, "Achieving near capacity on a multiple-antenna channel", IEEE Trans. Comm., vol. 51, no. 3, pp. 389-399, 2003.

[7]   G. J. Foschini and Michael. J. Gans, "On limits of wireless communications in a fading environment when using multiple antennas". Wireless Personal Communications. January 1998.

[8]   S. Lokya and A. Kouki, "New compound upper bound on MIMO channel capacity", IEEE Communication Letters, vol. 6, No. 3, 2002, pp 96-98.

[9]   S. Lokya, "Channel capacity of MIMO architecture using the exponential correlation matrix", IEEE Communication Letters, vol. 5, No 9, 2001. pp 369-371.

[10]   M. F. Demirkol, M. A. Ingram, Z. Yun, "Feasibility of closed loop operation for MIMO links with MIMO interference," Proc. of the IEEE Int'l Symp. on Antennas and Prop., Jun. 2004.

[11]   E. J. Ientilucci, "Using the Singular Value Decomposition", Chester F. Carlson Centre for Imaging Science, Rochester Institute of Technology, May 29, 2003.

[12]   A. Paulraj, R. Nabar and D. Gore, Introduction to Space-Time Wireless Communications, 2003, ISBN: 0-521-82615-2

[13]   C. Xiao and Y.R. Zheng, "On the Ergodic Capacity of MIMO Triply Selective Rayleigh Fading Channels",   IEEE Transactions on Wireless Communications, June 2008, Volume: 7 Issue: 6, pages: 2272 – 2279

[14]   S. Qiao, "Integer least squares: Sphere decoding and the LLL algorithm", Proceedings of C3S2E-08, ACM International Conference Proceedings Series, pp. 23-28, May 2008.

[15]   H. Vikalo, Sphere Decoding Algorithms for Digital Communications. PhD Thesis, Stanford University, 2003.

[16]   J.H. Conway and N.J. Sloane. Sphere Packings, Lattices and Graphs. Springer Verlag, 1993.

[17]   M. O. Damen, A. Chkeif, and J. C. Belfiore, "Lattice codes decoder for space-time codes", IEEE Communications Letters, 4:161{163, May 2000.

[18]   D. Landers and L. Rogge, "Identically distributed uncorrelated random variables not fulfilling the WLLN", Bull. Korean Math. Soc. 38 (2001), No. 3, pp. 605–610

[19]   I. Land, I. Graell, A. Amat, A. L.K. Rasmussen, "Bounding of MAP decode and forward relaying", 2010 IEEE International Symposium on Information Theory Proceedings (ISIT), pgs 938 – 942. June 2010.

[20]   L.L. Scharf. Statistical Signal Processing – Detection, Estimation and Time Series Analysis. Adison Wesley, 1991.

[21]   F. Li, L. Zhou, L. Liu, H. Li, "A quantum search based signal detection for MIMO-OFDM systems", Telecommunications (ICT), 2011 18th International Conference, pgs 276 - 281, 2011.

[22]   R. Sinha, A. Yener, R.D. Yates; "Non-coherent Multi-user Communications: Multistage Detection and Selective Filtering", EU RASIP Journal on Applied Signal Processing 2002:12, 1415–1426

[23]   Y. G. Li, N. Seshadri, and S. Ariyavisitakul, "Channel estimation for OFDM systems with transmitter diversity in mobile wireless channels," IEEE J. Select. Areas Commun., vol. 17, pp. 461–471, Mar. 1999.

[24]   Y. G. Li, J. H. Winters, and N. R. Sollenberger, "Signal detection for MIMO-OFDM wireless communications," IEEE Int. Conf. Commun., June 2001.

[25]   Y. G. Li, L. J. Cimini, Jr., and N. R. Sollenberger, "Robust channel estimation for OFDM systems with rapid dispersive fading channels," IEEE Trans. Commun., vol. 46, pp. 902–915, July 1998.

[26]   Institute of Electrical and Electronics Engineers, IEEE Standard 802.11a: Wireless LAN Medium Access Control (MAC) and Physical Layer (PHY) Specifications: High-Speed Physical Layer in the 5 GHz Band, 1999.

[27] Institute of Electrical and Electronics Engineers, IEEE Standard 802.11: Wireless Lan Medium Access Control (MAC) and Physical Layer (PHY) Specifications, Nov. 18, 1997.

[28] Institute of Electrical and Electronics Engineers, IEEE Standard 802.11g: Wireless LAN Medium Access Control (MAC) and Physical Layer (PHY) Specifications 2003.

[29] Institute of Electrical and Electronics Engineers, IEEE Candidate Standard 802.11n: Wireless LAN Medium Access Control (MAC) and Physical Layer (PHY)Specifications, 2004. [Online] http://grouper.ieee.org/groups/802/11/Reports

[30] K. Wai Wong, C. Ying Tsiu, R. S. Kwan Cheng, and W. Ho Mow, "A VLSI architecture of a K-best lattice decoding algorithm for MIMO channels," in Proc. IEEE International Symposium on Circuits and Systems (ISCAS '02), vol. 3, Scottsdale, AZ, USA, May 2002, pp. 273–276.

[31] Z. Guo and P. Nilsson, "A VLSI architecture of the Schnorr-Euchner decoder for MIMO systems," in Proc. IEEE 6th Circuits and Systems Symposium on Emerging Technologies: Frontiers of Mobile and Wireless Communication vol.1,Shanghai, China, June 2004, pp. 65–68.

[32] U. Fincke and M. Pohst, "Improved methods for calculating vectors of short length in a lattice, including a complexity analysis", Mathematics of Computation, vol. 44, pp. 463.471, April 1985.

[33]   P. Liu, I. Kim, "Exact and Closed-Form Error Performance Analysis for Hard MMSE-SIC Detection in MIMO Systems", IEEE Transactions on Communications, Issue 99, 2011.

[34]   E. Viterbo and E. Biglieri, "A universal lattice decoder," Colloq. GRETSI, pp. 611–614, September 1993.

[35]   S.Verdu, Multiuser Detection, Cambridge University Press, 1998.

[36]   C.P. Schnorr and M. Euchner, "Lattice basis reduction: improved practical algorithms and solving subset sum problems". Mathematical Programming, 66:181–191, 1994.

[37]   S.P. Alex; L.M.A. Jalloul, "Performance Evaluation of MIMO in IEEE 802.16e / WiMAX," IEEE Journal of Selected Topics in Signal Processing, vol.2, no.2, pp. 181–190, April 2008

[38]   F. Jelinek, "A fast sequential decoding algorithm using a stack", IBM Journal of Research and Development, 13:675–685, November 1969

[39]   E. Agrell, T. Eriksson, A. Vardy, and K. Zeger, "Closest Point Search in Lattices", IEEE Trans. on Information Theory, vol. 48, pp. 2201-2214, Aug. 2002.

[40]   M. O. Damen, H. El Gamal, G. Caire, "On Maximum-Likelihood Detection and the search for the closest lattice point", IEEE Transaction on Information Theory, vol. 49, pp. 2389-2401, Oct. 2003.

[41]   W. Abediseid and M.O. Damen, "On the Computational Complexity of Sphere Decoder for Lattice Space-Time Coded MIMO Channel", Department of Elect. & Comp. Engineering, University of Waterloo. March 2011.

[42]   L. Dong-Jin, K. Ryun-Woo, B. Youn-Shik, "Improved lattice reduction aided detection based on extended noise variance matrix for MIMO systems", Signal Processing Advances in Wireless Communications, pgs $1-5$, June 2007.

[43]   T. Ito, X.Wang, Y. Kakura, M. Madihian and A. Ushirokawa, "Performance comparison of MF and MMSE combined iterative soft interference canceller and V-BLAST technique in MIMO/OFDM systems," in *Proc. IEEE Veh. Technol. Conf.*, 2003, vol. 1, pp. 488–492.

[44]   T. Liu and Y. Liu, "Modified fast recursive algorithm for efficient MMSE-SIC detection of the V-BLAST system," *IEEE Trans. Wireless Commun.*, vol. 7, pp. 3713–3717, Oct. 2008.

[45]   T. Liu, "Some results for the fast MMSE-SIC detection in spatially multiplexed MIMO systems," IEEE Trans. Wireless Commun., vol. 8, pp. 5443–5448, Nov. 2009.

[46] P. Wolniansky, G. J. Foschini, G. D. Golden, and R. A. Valenzuela, "VBLAST: An architecture for realizing very high data rates over the rich scattering wireless channel," URSI International Symposium on Signals, Systems, and Electronics, ISSUE 98, 1998.

[47]   I. Barhumi, G. Leus, and M. Moonen, "Optimal training design for MIMO-OFDM systems in mobile wireless channels," IEEE Trans. Signal Processing, vol. 5, pp. 1615–1624, June 2003.

[48]   D. Hu, L. Yang, Y. Shi, and L. He, "Optimal Pilot Sequence Design for Channel Estimation in MIMO-OFDM Systems", IEEE Communication Letters, vol. 10, issue 1, Jan 2006.

[49] S. Yatawatta and A.P. Petropulu, "Blind Channel Estimation in MIMO-OFDM Systems with Multiuser Interference", IEEE Transactions on Signal Processing, vol. 54, no. 3, MARCH 2006.

[50] N. H. Dawod, I.D. Marsland and R.H. M. Hafez, "Improved Transmit Null Steering for MIMO–OFDM Downlinks with Distributed Base Station Antenna Arrays", IEEE Journal on Selected Areas in Communications, vol. 24, issue. 3, Mar 2006.

[51] S.M. Alamouti, "A simple transmitter diversity scheme for wireless communications", IEEE Journal on Selected Areas in Communications, vol. SAC-16, pp. 1451-1458, October 1998.

University of Hertfordshire, 2011

[52] T. Kashima, K. Fukawa, and H. Suzuki, "Adaptive MAP Receiver via the EM Algorithm and Message Passings for MIMO-OFDM Mobile Communications", IEEE Journal on Selected Areas in Communications, vol. 24, issue. 3, Mar 2006.

[53] B. L. Hughes, "Differential Space-time Modulation," IEEE Wireless Communications and Networking Conference, Vol. 1, pp. 145-149, 1999.

[54] G.D. Durgin, Space-time Wireless Channels, Prentice Hall PTR. Pearson Education, Inc. 2003.

[55] A. F. Naguib and A. R. Calderbank, "Space-time Coding and Signal Processing for High Data Rate Wireless Communications", Wireless Communications and Mobile Computing, Vol. 1, pp. 13-34, 2001.

[56] K. Fazel and L. Papke, "On the performance of Convolutionally-Coded CDMA/OFDM for mobile communication system", Proc. of PIMRC'93, pp. 468-472, September 1993.

[57] L. Zheng and D. Tse, "Diversity and multiplexing: A fundamental trade-off in multiple antenna channels", IEEE Transactions on Information Theory, vol. 49, pp. 1073 - 1096, May 2003.

[58] J. Luo, K. Pattipati, P. Willett and L. Brunel, "Branch-and-bound-based fast optimal algorithm for multiuser detection in synchronous CDMA," IEEE International Conference on Communications, vol. 5, pp. 3336-3340, 11-15 May 2003.

University of Hertfordshire, 2011

[59]   N. Al-Dhahir, C. Fragouli, A. Stamoulis, W. Younis, and R. Calderbank, "Space time processing for broadband wireless access," IEEE Communications Magazine, Volume: 40, Issue: 9, pp. 136-142, 2002

[60]   V. Tarokh, H. Jafarkhani, and A. R. Calderbank, "Space-time Codes for High Data Rate Wireless Communication: Performance Criterion and Code Construction," IEEE Trans. Inform. Theory, Vol. 44, No. 2, pp. 744-765, July 1998

[61]   G. H. Golub and C. F. Van Loan, Matrix Computations, 3rd ed. Baltimore: Johns Hopkins University Press, 1996.

[62]   E. Biglieri, G. Taricco, and A. Tulino, "Performance of space-time codes for a large number of antennas," IEEE on IT, vol. 48, no. 9, pp. 1794–1803, 2002.

[63]   D.A. Gore, J. R. W. Heath, and A.J. Paulraj, "Transmit selection in spatial multiplexing systems," IEEE Comm. Letters, vol. 6, no. 11, pp. 491–493, November 2002.

[64]   U. Fincke and M. Phost, "Improved methods for calculating vectors of short length in a lattice, including a complexity analysis," Math. Comp., vol. 44, pp. 463–471, April 1985.

[65] M. Damen, A. Chkeif, and J. Belfiore, "Lattice code decoder for space-time codes," IEEE Comm. Letters, vol. 4, no. 5, pp. 161–163, May 2000.

[66] J. G. Proakis, Digital Communications, 4th Ed, McGraw-Hill, New York, 2001.

[67] R. van Nee, R. Prasad, OFDM wireless multimedia communications, Boston: Artech House, 2000.

[68] K. Yen and L. Hanzo, "Genetic-algorithm-assisted multiuser detection in asynchronous CDMA communications", IEEE Trans. Veh. Technol., vol. 53, no. 5, pp. 1413–1422, Sep. 2004.

[69] X. Wu, T. C. Chuah, B. S. Sharif, and O. R. Hinton, "Adaptive robust detection for CDMA using a genetic algorithm," Inst. Electr. Eng. Communications, vol. 150, pp. 437–444, Dec. 10, 2003.

[70] A. F. Molisch, Wireless Communications. Wiley & Sons, 2005

[71] J. Boutros, "Lattice codes for Rayleigh fading channels," Theses de Doctorat, ENST, Paris, June 1996.

[72] J. Boutros and E. Viterbo, "Signal space diversity: a power and bandwidth efficient diversity technique for the Rayleigh fading channel," IEEE Transactions on Information Theory, vol. 44, pp. 1453-1467, July 1998.

[73]   L. Brunel, "Optimum multiuser detection for MC-CDMA systems using sphere decoding," PIMRC'01, San Diego, California, October 2001.

[74]   L. Brunel, "Optimum and sub-optimum multiuser detection based on sphere decoding for Multi-Carrier Code Division Multiple Access systems," ICC'02, New York, April 2002.

[75]   L. Brunel and J. Boutros, "Lattice decoding for joint detection in direct sequence CDMA systems", IEEE Transactions on Information Theory, vol. 49, no. 4, pp. 1030-1037, April 2003.

[76]   G. Caire, G. Taricco and E. Biglieri, "Bit-interleaved coded modulation, "IEEE Transactions on Information Theory", vol. 44, no. 3, pp. 927-946, May 1998.

[77]   T. Cui and C. Tellambura, "Joint channel estimation and data detection for OFDM systems via sphere decoding", Proc. IEEE Global Telecommunications Conf, Nov. 2004, vol. 6, pp. 3656–3660.

[78]   T. Cui and C. Tellambura, "Approximate ML detection for MIMO systems using multistage sphere decoding", IEEE Signal Process. Lett., vol. 12, no. 3, pp. 222–225, Mar. 2005.

[79]   M. Stojnic, B. Hassibi and H. Vikalo, "A branch and bound approach to speed up the sphere decoder," Proc. IEEE ICASSP 2005, pp. 429–433, May 2005.

University of Hertfordshire, 2011

[80]   J. Boutros, F. Boixadera and C. Lamy, "Bit-interleaved coded modulations for multiple input multiple output channels," Proc. of the IEEE 6th International Symposium on Spread Spectrum Techniques & Applications, New Jersey, September 2000.

[81]   M. Jiang, J. Akhtman, F. Guo, and L. Hanzo, "Iterative joint channel estimation and multi-user detection for high-throughput multiple antenna aided OFDM systems", Proc. 2006 IEEE 63rd Vehicular Technology Conf. (VTC '06 Spring), Melbourne, Australia, May 7–10, 2006.

[82]   C.-T. Chiang and C.-Y. Chang, "An improved genetic algorithm based on eugenic population for multiuser detection in DS-CDMA systems", Proc. IEEE, Annual Int. Conf. (TENCON), Beijing, China, Oct. 28–31, 2002, vol. 2, pp. 984–987.

[83]   A. Wolfgang, N. N. Ahmad, S. Chen, and L. Hanzo, Genetic algorithm assisted minimum bit-error rate beamforming", Proc. IEEE Vehicular Technology Conf. (VTC Spring), Milan, Italy, May 17–19, 2004, pp. 142–146.

[84]   M. Y. Alias, S. Chen, and L. Hanzo, "Genetic algorithm assisted minimum bit-error rate multiuser detection in multiple antenna aided OFDM", Proc. IEEE Vehicular Technology Conf. (VTC-Fall), Los Angeles, CA, Sep. 2004, pp. 548–552.

[85]   X. Li and J.A. Ritcey, "Bit-interleaved coded modulation with iterative decoding", IEEE Communications Letters, vol. 1, no. 6, November 1997.

[86] W. Ledermann and E. Lloyd, Handbook of Applicable Mathematics, Volume II: Probability. New York: Wiley, 1980.

[87] G. Gelli, L. Paura, and A. Ragozini, "Blind widely linear multiuser detection," IEEE Communication Letters., vol. 4, pp. 187–189, Jun. 2000.

[88] S. Kay, Fundamentals of Statistical Signal Processing. Englewood Cliffs, NJ: Prentice-Hall, 1998.

[89] A. Murugan, H. Gamal, M. Damen, and G. Caire, "A unified framework for tree search decoding: Rediscovering the sequential decoder," *IEEE Trans. Inf. Theory*, vol. 52, no. 3, pp. 933–953, Mar. 2006.

[90] E. Agrell, J. Lassing, E.G. Strom and T. Ottosson, "On the optimality of the binary reflected Gray code", IEEE Transactions on Information Theory, 2004.

[91] J. Jalden and B. Ottersten, "On the complexity of sphere decoding in digital communications," *IEEE Trans. Signal Process.*, vol. 53, 4, no. 4, pp. 1474–1484, Apr. 2005.

[92] Q. H. Spencer et al., "An Introduction to the Multi-User MIMO Downlink" IEEE Commun. Mag., vol. 42, no. 10, Oct. 2004, pp. 60–67.

[93] B. C. B. Peel, B. M. Hochwald, and A. L. Swindlehurst, "A Vector-Perturbation Technique for Near-Capacity Multi antenna Multiuser Communication, Part I: Channel Inversion and Regularization," *IEEE Trans. Commun.*, vol. 53, Jan. 2005, pp. 195–202.

[94] H. Bolcskei, D. Gesbert, and A. J. Paulraj, "On the capacity of OFDM based spatial multiplexing systems", IEEE Trans. Communications., vol. 50, no. 2, pp. 225- 234, Feb. 2002.

[95] C. Studer, M. Wenk, A. Burg, and H. Bolcskei, "Soft Output Sphere Decoding: Performance and Implementation Aspects", ASSC '06 Fortieth Asilomar Conference on Signals, Systems and Computers, 2006.

[96] N. Jindal, "MIMO Broadcast Channels with Finite-Rate Feedback," IEEE Trans. Info. Theory, vol. 52, July 2006, pp. 5045–60.

[97] Z. Wang and G. B. Giannakis, "Wireless Multicarrier Communications", Signal Processing Mag., pp. 29–48, May 2000.

[98] M. C. Necker and G. L. Stuber, "Totally blind channel estimation for OFDM on fast varying mobile radio channels", IEEE Trans. Wireless Commun., vol. 3, no. 5, pp. 1514–1525, Sep. 2004.

[99] W. C. Chung, N. J. Aug., and D. S. Ha, "Signaling and Multiple Access Techniques for ultra wideband 4G Wireless Communication Systems", Wireless Commun., vol. 12, pp. 46–55, Apr. 2005.

University of Hertfordshire, 2011

[100] X. Zhu and R. D. Murch, "Layered space-frequency equalization in a single-carrier MIMO system for frequency-selective channels", IEEE Trans. Wireless Commun., vol. 3, no. 3, pp. 701–708, May 2004.